Journal of Molecular Structure 1200 (2020) 127097

Contents lists available at ScienceDirect

Journal of Molecular Structure

journal homepage: http://www.elsevier.com/locate/molstruc

Synthesis and evaluation of new 4(3*H*)-Quinazolinone derivatives as potential anticancer agents

Srikanth Gatadi [a], Gauthami Pulivendala [b], Jitendra Gour [a], Satyaveni Malasala [a], Sushmitha Bujji [a], Ramulu Parupalli [a], Mujahid Shaikh [a], Chandraiah Godugu [b], Srinivas Nanduri [a, *]

[a] Department of Medicinal Chemistry, National Institute of Pharmaceutical Education and Research (NIPER), Hyderabad, 500 037, India
[b] Department of Pharmacology and Toxicology, National Institute of Pharmaceutical Education and Research (NIPER), Hyderabad, 500 037, India

ARTICLE INFO

Article history:
Received 11 June 2019
Received in revised form
18 September 2019
Accepted 19 September 2019
Available online 19 September 2019

Keywords:
4(3*H*)-quinazolinone
Cytotoxicity
MDA-MB-231
Cell migration
Colony formation

ABSTRACT

A series of new 4(3*H*)-quinazolinones were synthesized and evaluated for their cytotoxic activity against a set of human cancer cell lines MDA-MB-231 and MCF-7 (breast), HCT-116 and HT-29 (colon) and A549 (lung). Among the tested compounds, **22a** exhibited promising cytotoxic activity against MDA-MB-231 (IC_{50}: 3.21 μM) and HT-29 (IC_{50}: 7.23 μM) cell lines. The mechanism of action and the apoptosis inducing effect of the compound **22a** were studied using the breast cancer cell line MDA-MB-231. Treatment of MDA-MB-231 cell line with compound **22a** showed typical apoptotic morphology like cell shrinkage, chromatin condensation and horseshoe shaped nuclei formation. Flow cytometric analysis indicated that the compound induces G0/G1 phase of cell cycle arrest in a dose dependent manner. The binding modes of the potent compounds with EGFR target protein were investigated by docking studies.

1. Introduction

Cancer is a hyper proliferative disease with the potential to invade to other parts of the body [1]. As the current chemotherapeutic agents are not sufficient to tackle the spread of this dreadful disease [2], search for new chemotherapeutic agents which can arrest cell proliferation are being explored. In the quest for new anticancer agents, efforts have been focused on the development of compounds with 4(3*H*)-quinazolinone heterocycle. 4(3*H*)-Quinazolinone is a privileged structure possessing wide range of biological properties such as anticancer, antimicrobial, anti-inflammatory and anticonvulsant activities. *etc* [3–8]. Idelalisib **I**, a quinazolinone based drug used for the treatment of certain hematological malignancies acts as a phosphoinositide-3-kinase inhibitor [9,10]. Canertinib **II** is used as an experimental drug candidate for the treatment of cancer [11]. Cao et al. [12] reported the *in vitro* antitumor activity of 4(3*H*)-quinazolinones with dithiocarbamate side chains **III**. Al-Rashood et al. [13] reported a series of compounds **IV** with both antitumor potency and DHFR inhibition. Raffa et al. [14] reported the cytotoxic properties of new 2-styrylquinazolinone derivatives **V**. Suwaidan and co-workers reported a novel series of 3-benzyl-substituted-4(3*H*)-quinazolinones **VI** as potential anti-tumor agents [15] (Fig. 1).

Additionally, several Quinazolinone based compounds have been shown to exert their anti-cancer activity through EGFR kinase inhibition. Erlotinib **VII** [16], used for the treatment of non-small cell lung cancer and pancreatic cancer acts on the epidermal growth factor receptor (EGFR). Lapatinib **VIII** [17], an orally active drug for breast cancer and other solid tumours is found to be a dual tyrosine kinase inhibitor interfering with the HER2/neu and epidermal growth factor receptor (EGFR) pathways. Yin et al. [18] reported the anticancer potential of new EGFR/HER2 dual inhibitors bearing an oxazolo[4,5-g]quinazolin-2(1*H*)-one moiety **IX**. Tsou et al. [19] reported a series of new 6-substituted-4-(3-bromophenylamino)quinazoline derivatives **X** that might function as irreversible inhibitors of EGFR and human epidermal growth factor receptor (HER-2) tyrosine kinases. Soliman et al. [20] explored a series of new *N*-alkyl-2-[(4-oxo-3-(4-sulfamoylphenyl)-3,4-dihydroquinazolin-2-yl)thio]acetamide derivatives **XI** as anticancer agents. Soliman et al. [21] also reported the series of new sulphonamide benzoquinazolinones **XII** as dual EGFR/HER2 inhibitors (Fig. 2).

* Corresponding author.
E-mail address: nandurisrini92@gmail.com (S. Nanduri).

https://doi.org/10.1016/j.molstruc.2019.127097
0022-2860/

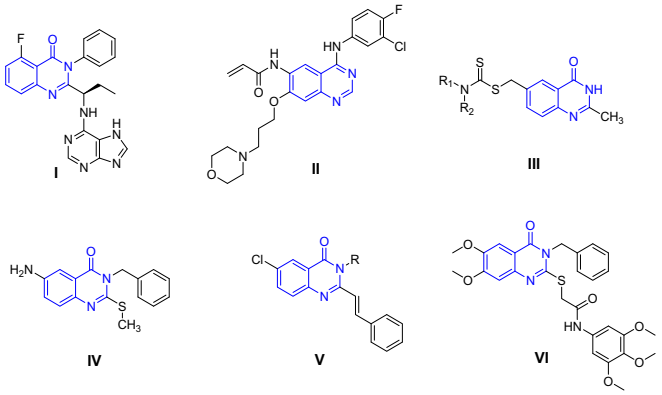

Fig. 1. Structure of some reported bioactive quinazolinones as anticancer agents.

On the other hand, 1,2,3-triazole (Fig. 3) could also be considered as an important scaffold due to its high stability, hydrogen bonding ability and broad applicability in medicinal chemistry [22]. In recent years, researchers have increasingly focused on its anticancer potential. Duan et al. [23] reported the 1,2,3-triazole-dithiocarbamate hybrids **XIII** as potential anticancer agents. Kamal et al. [24] reported the anticancer properties of new 1,2,3-triazole-linked pyrrolobenzodiazepine conjugates **XIV**. Recently, Sumit and co-workers reported a series of new 1*H*-1,2,3-triazole tethered nitroimidazole−isatin conjugates **XV** as potent anti-cancer agents [25].

Hybridization of the two dissimilar bioactive pharmacophores in a single molecule is a frequently used approach for the exploration of novel compounds which may have synergistic effect [26]. In the current work, we have designed and synthesized new 1,2,3-

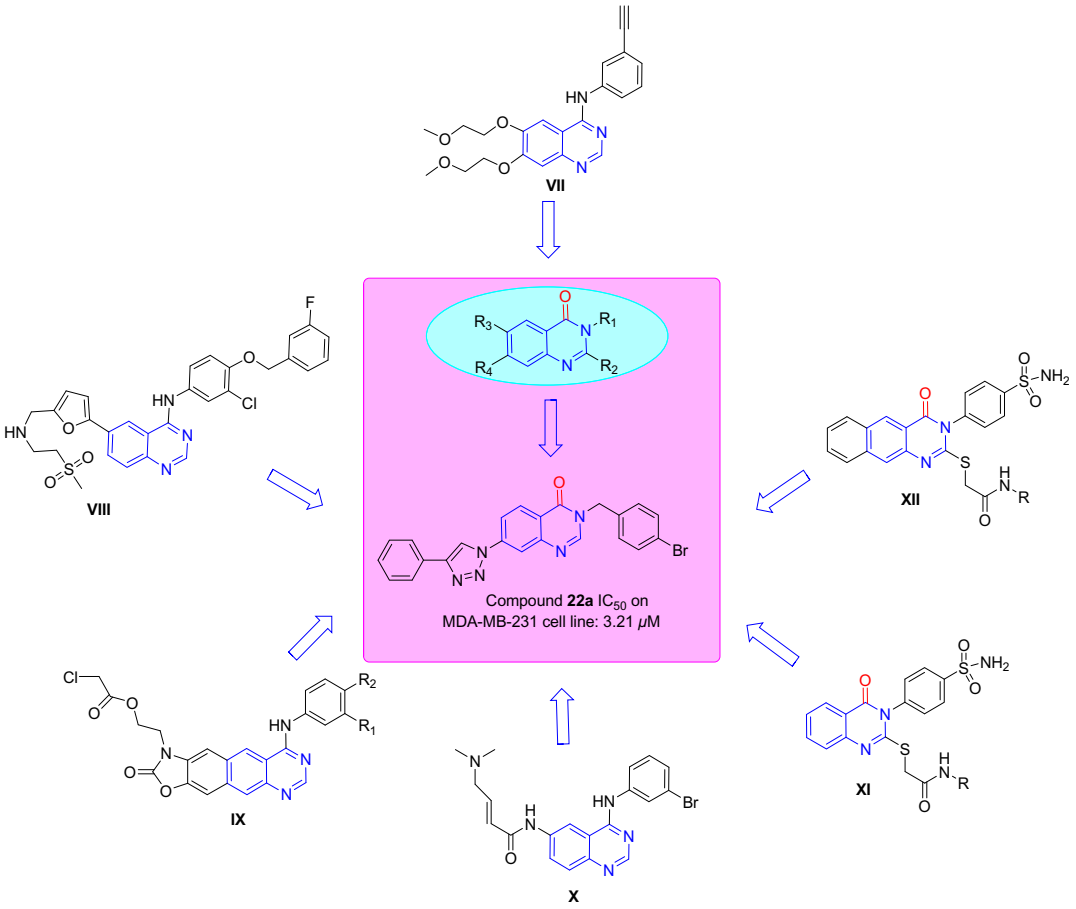

Fig. 2. Design of 4(3*H*)-Quinazolinone derivatives as new EGFR inhibitors.

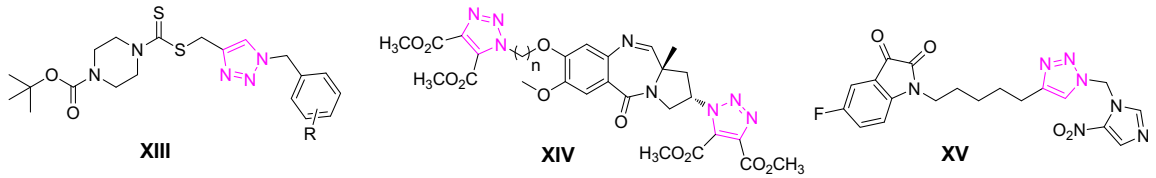

Fig. 3. Structure of some reported bioactive 1,2,3-triazoles as anticancer agents.

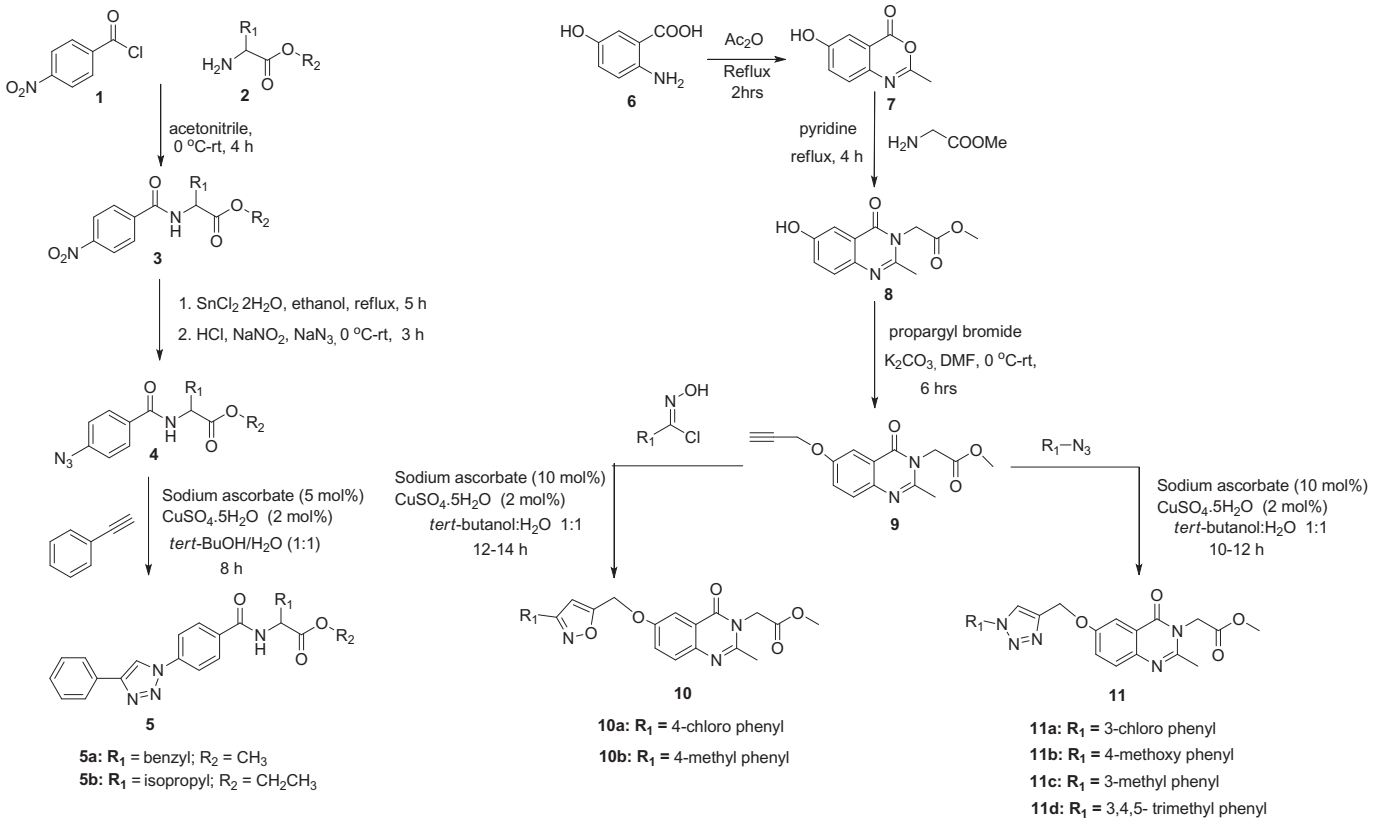

Scheme 1. Synthesis of 4-(4-phenyl-1*H*-1,2,3-triazol-1-yl)benzamide **5a-5b** and methyl 2-(2-methyl-4-oxoquinazolin-3(4*H*)-yl)acetate **10a-10b, 11a-11d** derivatives.

triazole linked 4(3*H*)-quinazolinone and also some benzamido acetate derivatives and evaluated them for their cytotoxic potential against a number of human cancer cell lines. We have also studied their binding affinity to EGFR protein kinase through molecular docking studies.

2. Results and discussion

2.1. Chemistry

A series of new 1,2,3-triazolylbenzamido acetate derivatives were synthesized as shown in Scheme 1. 4-nitro benzoyl chloride **1** and amino acid ester **2** were reacted in acetonitrile at room temperature to afford the intermediate **3**. The nitro group in intermediate **3**, was reduced in the presence of tin(II)chloride under reflux conditions in ethanol. Further, the obtained aniline derivative was allowed to undergo azidation reaction using sodium nitrite and sodium azide in 2N HCl to afford the azide intermediate **4**. Finally, alkyl 2-(4-(4-phenyl-1*H*-1,2,3-triazol-1-yl)benzamido)acetate derivatives **5a-5b** were synthesized by reacting the azide intermediate **4** with phenylacetylene by employing Cu(I)-catalyzed azide-alkyne cycloaddition (CuAAC) reaction.

Besides, a series of new quinazolin-4(3*H*)-one derivatives were synthesized as shown in Schemes 1, **2** & **3**. 5-hydroxy anthranilic acid **6** were converted into benzoxazinone intermediate 7 by treating with acetic anhydride under reflux for 2 h. The benzoxazinone intermediate **7** was dissolved in pyridine and glycine ester was added and the reaction mixture was refluxed for 4–5 h to give the corresponding methyl 2-(6-hydroxy-2-methyl-4-oxoquinazolin-3(4*H*)-yl)acetate **8**. The intermediate **8** was subjected to *O*-propargylation by using propargyl bromide to afford corresponding 5-*O*-propargylated quinazolinone derivative **9**. Treatment of **9** with various substituted azides under click conditions gave the corresponding triazole derivatives **11a-11d**. When the intermediate **9** was reacted with oxime gave isoxazole derivatives **10a** and **10b (Scheme 1).**

Similarly, when a mixture of benzoxazinone intermediate **7** and substituted benzylamine in glacial acetic acid were refluxed, it yielded 3-benzyl-6-hydroxy-2-methylquinazolin-4(3*H*)-one derivative **14** in moderate to good yields (Scheme 2). The intermediate **14** was further subjected to *O*-propargylation by using propargyl-bromide to afford corresponding 5-*O*-propargylated quinazolinone derivative **15.** Treatment of **15** with various substituted azides under click conditions gave the corresponding triazole derivatives **16a-16j**. Further, intermediates **16a** & **16b** were reacted with 4-cyano benzaldehyde in glacial acetic acid under reflux conditions for overnight to afford the new 2-styrylquinazolin-4(3*H*)-one derivatives **17a & 17b** as final compounds (Scheme 2) in moderate to excellent yields.

In Scheme 3, the 4 or 5-nitro anthranilic acid **18** was reacted with formamide at room temperature to afford 6 or 7-nitroquinazolin-4(3*H*)-one intermediates **19**. Further, the intermediates were treated with substituted benzyl bromide in presence of sodium hydride as base in dry DMF at room temperature to afford 6 or 7-nitro 3-benzylquinazolin-4(3*H*)-one derivatives **20**. The intermediate **20** was further converted into **21** by reduction of the nitro group in **20** with tin(II) chloride under reflux conditions in ethanol and subsequent azidation reaction using sodium nitrite and sodium azide in 2N HCl. Synthesis of the designed compounds **22a-22b, 22'a** and **23a-23d** were accomplished by reacting the azide intermediate 6 or 7-azido-3-benzylquinazolin-4(3*H*)-one **21** with various substituted phenylacetylenes or phenoxymethylacetylene by employing Cu(I)-catalyzed azide-alkyne cycloaddition (CuAAC) reaction [27–29]. Structures of all the newly

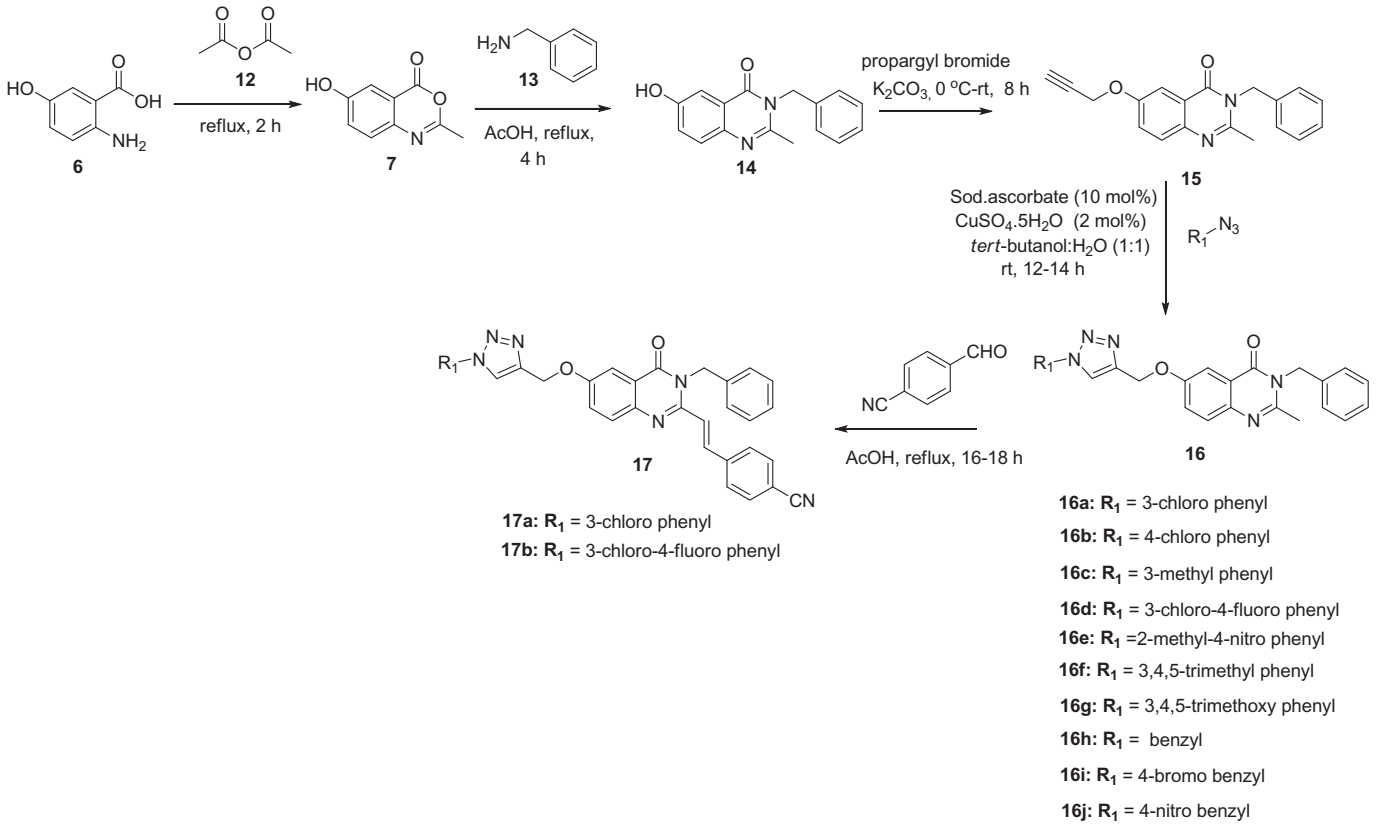

Scheme 2. Synthesis of 6-((1*H*-1,2,3-triazol-4-yl)methoxy)-3-benzylquinazolin-4(3*H*)-one derivatives **16a**–**16j** & **17a-17b**.

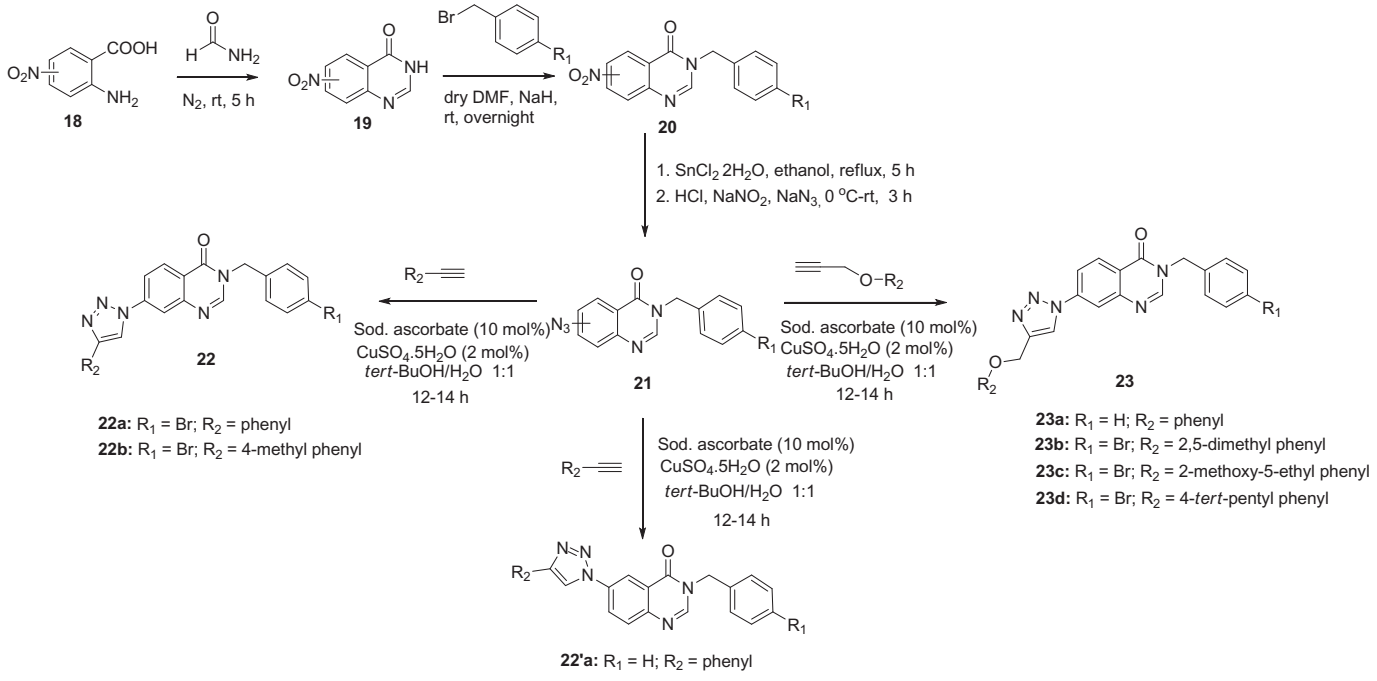

Scheme 3. Synthesis of 3-benzyl-7-(1*H*-1,2,3-triazol-1-yl)quinazolin-4(3*H*)-one derivatives **22a**-**22b**, **22'a**, and **23a-23d**.

synthesized compounds were confirmed by ^{1}H NMR, ^{13}C NMR and HRMS (ESI) spectroscopic techniques.

3. Pharmacology

3.1. In vitro cytotoxic activity

The newly synthesized quinazolin-4(3*H*)-one derivatives were screened for their cytotoxic activity against human cancer cell lines MDA-MB-231 and MCF-7 (breast), HCT-116 and HT-29 (colon) and A549 (lung), using 3-(4,5-dimethylthiazol-2-yl)-2,5-diphenyltetrazolium bromide (MTT) assay [30]. IC_{50} value is defined as the concentration required to cause 50% inhibition of cancer cell growth. The IC_{50} (μM) values of the test compounds **5a-5b**, **10a-10b**, **11a-11d**, **16a-16j**, **17a-17b, 22a-22b**, **22'a**, **23a-23d** are given in Table 1. Doxorubicin is used as the positive control. The results indicated that some of the synthesized compounds possessed moderate to potent growth inhibition against the tested cancer cells. Among the tested compounds, compound **22a** exhibited potent cytotoxic activity against HT-29 & MDA-MB-231 cell lines with IC_{50} of 7.29 μM and 3.21 μM values respectively. It is significant to note that the IC_{50} of Doxorubicin (3.77 μM) is comparable to the IC_{50} value of **22a** against MDA-MB-231 cell line. The promising cytotoxic activity of compound **22a** on MDA-MB-231 cancer cells encouraged us to study its effects at cellular level.

3.2. In vitro cell migration assay/wound healing assay

Cell migration is a central and integral process of various important biological mechanisms like tissue development, tissue wound healing and pathological conditions like cancer. Uncontrolled cell migration is the first step and hallmark of cancer cell metastasis, which is composed of sequential events called metastatic cascade [31]. Given the importance of cell migration in pathobiology of cancer, we have investigated the effect of compound **22a** on MDA-MB-231 cells by performing wound scratch assay. In order the evaluate the effect of **22a** on cell motility, an artificial wound was created in culture well plate with confluent monolayer of cells using sterile tip as described in section 6.3. As depicted in Fig. 4, it was observed that artificially created wound was closed in control cells reflecting the rapid proliferation and migratory property of cancer cells. Furthermore, **22a** treated cells showed significant inhibition of cell migration into the wound area. A concentration dependent effect was observed where the low dose (2 μM) showed partial closure of the denuded area, mid dose (4 μM) treatment showed wound mild closure where as the highest dose of 6 μM displayed conspicuous suppression of cell migration as evident from the scantly present cells in the denuded area. These results suggest the potential of **22a** inhibition migration and motility of cancer cells.

Table 1
IC_{50} values (μM) of the tested compounds against selected human cancer cell lines.

Compound name	HCT-116	HT-29	A549	MDA-MB-231	MCF-7
5a	>30	>30	>30	>30	>30
5b	>30	>30	>30	>30	>30
10a	>30	>30	>30	>30	>30
10b	>30	>30	>30	>30	>30
11a	>30	>30	>30	>30	>30
11b	>30	>30	>30	**29.34**	>30
11c	>30	>30	>30	>30	>30
11d	>30	**10.82**	>30	**16.57**	>30
16a	>30	>30	>30	>30	>30
16b	>30	>30	>30	>30	>30
16c	>30	>30	>30	>30	>30
16d	>30	>30	>30	>30	>30
16e	>30	>30	>30	>30	>30
16f	>30	>30	>30	>30	>30
16g	>30	>30	>30	>30	>30
16h	>30	>30	>30	**5.74**	>30
16i	>30	>30	>30	>30	>30
16j	>30	>30	>30	>30	>30
17a	>30	>30	>30	>30	>30
17b	>30	>30	>30	**12.57**	>30
22a	>30	**7.23**	>30	**3.21**	>30
22b	>30	>30	>30	>30	>30
22'a	>30	>30	>30	>30	13.50
23a	>30	>30	>30	>30	>30
23b	>30	>30	**9.01**	**14.49**	>30
23c	>30	>30	>30	>30	>30
23d	>30	>30	>30	>30	>30
DOX	7.53	9.56	3.95	3.77	0.32

IC_{50} values are the concentrations that cause 50% inhibition of cancer cell growth. breast (MDA-MB-231 and MCF-7), colon (HCT-116 and HT-29), lung (A549) DOX: Doxorubicin as reference standard.

3.3. Acridine orange–ethidium bromide (AO–EB) staining

AO/EB staining is dual fluorescent staining assay commonly used to detect tumor cell apoptosis. AO/EB staining identifies apoptosis and necrotic-associated changes occurring in cell membranes. This assay distinguishes viable cells from the non-viable ones based upon the cell membrane integrity [32]. Changes pertaining to apoptotic cell death upon treatment with **22a** were thus studied by AO/EB staining. AO is up-taken by cells with intact cell membrane and is visualized as green fluorescence. Viable cells are impermeable to EB and can be taken up by cells with loss of membrane integrity Therefore, early apoptotic cells have bright green nucleus with condensed chromatin and fragmented nuclei; and late apoptotic cells show orange colored condensed and fragmented chromatin. Cell death due to necrosis is visualized as a structurally normal orange nucleus. From Fig. 5, untreated cells did not show any morphological changes pertaining to apoptosis/necrosis. Cells treated with **22a** showed significant apoptosis changes characterized by bright green dots representing chromatic condensation. Concentration dependent increase in apoptosis was apparent upon treatment with **22a**. Also, both doses showed chromatin condensation and blebbing in cells treated with **22a**.

3.4. DAPI staining

4,6-Diamidino-2-phenylindole (DAPI) is a fluorescent dye which specifically binds to adenine-thymine clusters of double stranded DNA and stains it blue. Healthy cells display intact round nuclei with distinct margins upon staining with DAPI, where as apoptotic cells show intense blue fluorescence as compared to nuclei of healthy cells [33]. Additionally, condensed chromosome and nuclear fragmentation are apparent in apoptotic cells. The results from the Fig. 6 clearly demonstrated that the nuclear structure of untreated cells showed normal round nuclei whereas **22a** treated cells exhibited nuclear fragmentation, condensed chromosome and the characteristic pyknotic, horse shoe pattern of the nuclei. The high concentration treated cells showed higher degree of apoptosis as evidenced by the increased number of horseshoe shaped nuclei.

3.5. Colony forming assay

Colony formation assay or clonogenic assay is an *in vitro* cell survival assay which is based on the ability of a single cell to form into colony of cells through unhampered cell proliferation [34]. Clonogenic assay also evaluated the retention/loss of reproductive integrity of a cell upon treatment with a cytotoxic compound. From the Fig. 7, treatment with compound **22a** at different

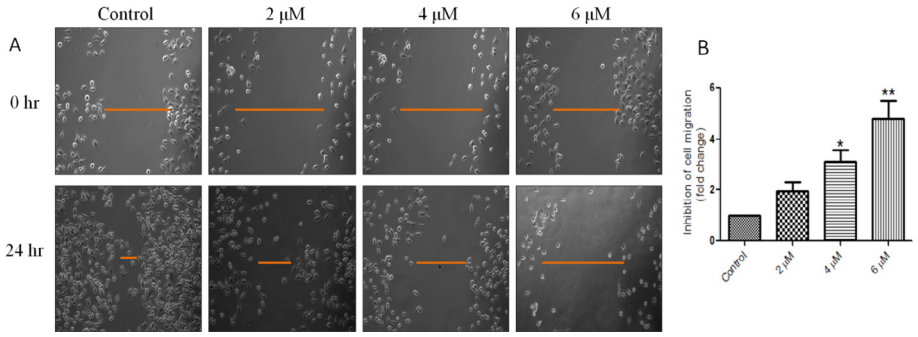

Fig. 4. (A) Representative microphotographs of cell migration assay of all experimental groups at 0 h and 24 h (Magnification 10×). Treated wells show reduction in migration of cells into the artificially created wound (B) Graphical representation of inhibition in cell migration upon treatment with **22a** at different concentrations. *p < 0.05 and **p < 0.01 of control vs. **22a** treatment.

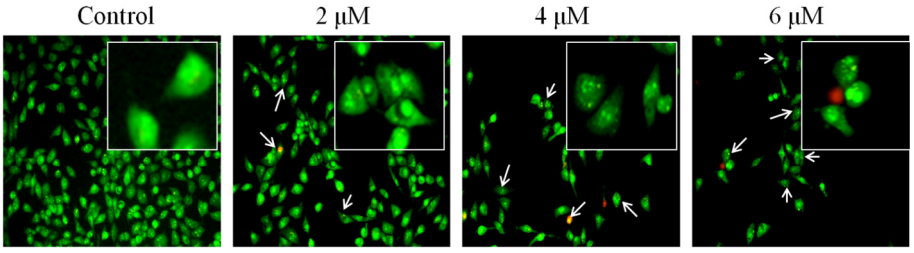

Fig. 5. Representative microphotographs of apoptosis induction by **22a** in MDA-MB-231 cells using AO/EB staining (Magnification 20×). Untreated cells exhibiting normal green structure with distinct nucleus, whereas treatment with 22a showed dose dependent induction of apoptosis as evident from membrane blebbing and apoptotic bodies. White arrows indicate the altered cell/nuclei morphological changes.

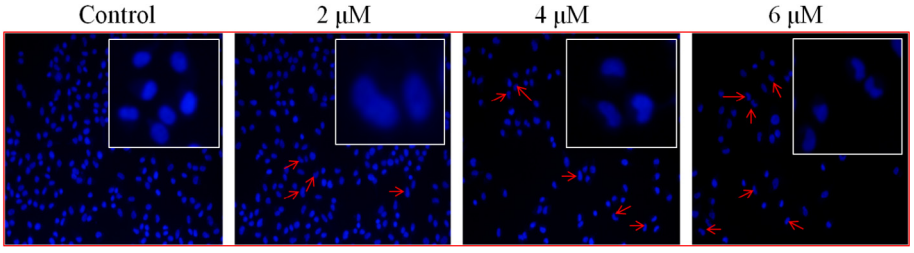

Fig. 6. Representative microphotographs of morphological changes in nuclei of untreated cells and as a result of treatment with **22a** in MDA-MB-231 cells as indicated by DAPI staining (Magnification 20×). Untreated cells show normal oblong and distinct nuclei. **22a** treated cells indicating shrinked, horse shoe nucleus, fragmentation and pyknotic nucleus of the cells. The arrows indicate the nuclear morphological changes induced by **22a**.

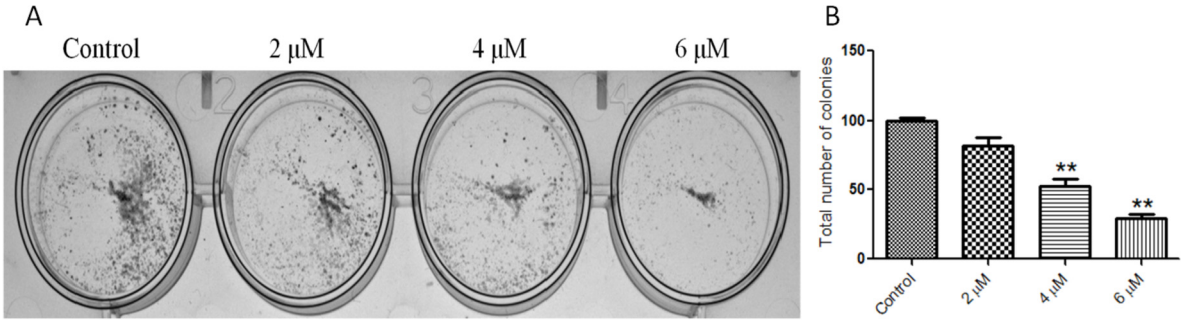

Fig. 7. (A) Image displaying the effect of **22a** at various concentrations of 2, 4 and 6 μM on colony formation of MDA-MB-231 cells (B) Graphical representation of number of colonies of MDA-MB-231 cells in control and treated culture wells. **p < 0.01 of control vs. 22a treatment.

concentrations of 2, 4 and 6 μM exhibited a concentration dependent inhibition of proliferation and colony formation. The total colonies were represented as a total number of colonies vs. concentration.

3.6. Cell cycle analysis

Most of the chemotherapeutic compounds exert their cytotoxic effect either by induction of apoptosis or by arresting cell cycle at a

specific checkpoint [35]. The inappropriate regulation of cell cycle by anticancer agent has been considered to be an effective strategy in the development of new cancer therapeutics. Therefore, it was our interest to examine the effect of compound **22a** on cell cycle progression of MDA-MB-231 cell by using flow cytometry analysis method [36]. The mechanism by which **22a** inhibited cell growth was studied by performing cell cycle analysis. Cells were treated with **22a** for 24 h at concentrations of 4 and 6 μM. Results from the Fig. 8 clearly demonstrated the accumulation of cells in G0/G1 phase from 61.88% in untreated cells to 67.61% and 68.43% in 4 and 6 μM respectively. These results clearly indicated that the treatment of **22a** led to G0/G1phase of cell cycle arrest. Though there was apparent increase in the percentage of cells arrested in G0/G1 phase upon treatment with **22a** at both the doses, the difference was not significant.

4. Molecular docking studies

With a view to throw light on the probable protein target of the newly synthesized quinazolinone derivatives, we have performed their interactions studies with EGFR (PDB ID: 1XKK) binding site [37]. The new representative compounds 11d, 16h, 22a and 23b were docked against EGFR protein. Ligand interactions showed that the compounds exhibited good interactions with glide scores ranging from −6.033 to −7.386 against EGFR target protein. The studies revealed that the 4-bromo of 3-*N*-benzyl moiety in the most potent compound **22a** exhibited hydrogen bonding interaction with active site residue TYR998 and aromatic hydrogen bonding interaction between phenyl ring system and ASP855 with good docking score. Compound **23b** exhibited aromatic hydrogen bonding interactions between aromatic phenyl moieties and residues VAL717, LEU718 and ASP 855 of EGFR target protein (Fig. 9).

5. Conclusion

In conclusion, a series of new quinazolin-4(3*H*)-ones have been synthesized and evaluated for their cytotoxic activity against selected human cancer cell lines *viz.* colon (HCT-116 and HT-29), breast (MDA-MB-231 and MCF-7) and lung (A549). Among all the tested compounds, **22a** exhibited potent cytotoxic activity with IC_{50} value of 3.21 μM against MDA-MB-231 cell line. The exposure of compound **22a** to MDA-MB-231 cells resulted in G0/G1 phase of cell cycle arrest and inhibition of *in vitro* cell migration. The apoptosis inducing effect of **22a** was further analysed by acridine orange/ethidium bromide (AO-EB) staining and DAPI staining. Molecular docking studies of these compounds with EGFR protein showed good binding affinities, suggesting that these compounds act as EGFR Kinase inhibitors. The ease of synthesis and good anticancer potential of these compounds makes them acceptable starting points for the development of new chemotherapeutic agents.

6. Materials & methods

All the chemicals, reagents and starting materials were obtained from commercial available providers and were used as such. The monitoring of all the reactions were performed by thin layer chromatography (TLC-MERCK pre-coated silica gel 60-F254 aluminium plates) under UV light. Melting points were checked using Stuart® SMP30 apparatus and are uncorrected. ^{1}H and ^{13}C NMR were performed on Bruker Advance 500 MHz spectrometer using tetramethylsilane (TMS) as the internal standard and chemical shifts are reported in ppm. Chemical shifts are referenced to TMS (δ 0.00 for ^{1}H NMR and ^{13}C NMR), $CDCl_3$ (δ 7.26 for ^{1}H NMR and 77.00 or 77.16 for ^{13}C NMR) or DMSO→d_6 (δ 2.50 for ^{1}H NMR and 39.7 for ^{13}C NMR) or combination of $CDCl_3$ and DMSO-d_6, in which DMSO-d_6 was used as an internal reference or trifluoroacetic acid-d (δ 164.2 and δ 116.6 for ^{13}C NMR). Spin multiplicities are reported as s (singlet), d (doublet), dd (double doublet), t (triplet) and m (multiplet). Coupling constant (*J*) values are reported in hertz (Hz). HRMS were determined with Agilent QTOF mass spectrometer 6540 series instrument and were performed in the ESI techniques at 70 eV. Column chromatography was performed using silica gel 60−120 or 100−200 mesh.

Intermediates **3**, **4**, **7**, **8**, **14** (Scheme 1 & **2**) were prepared according to the procedures described in literature [27,28].

6.1. General reaction procedure for the synthesis of 4-(4-phenyl-1H-1,2,3-triazol-1-yl)benzamide derivatives ***5a-5b***

Compound (**4**, 2 mmol) (Scheme 1) and phenylacetylene (2 mmol) were suspended in 10 mL of a 1:1 *tert*-BuOH/H_2O mixture. To the heterogeneous mixture, sodium ascorbate (5 mol%), copper(II)sulfate pentahydrate (2 mol%) were added and the reaction mixture was allowed to stir for 8 h to give crude white or pale yellow precipitates, which were filtered, washed with water, followed by hexane and finally purified by using column chromatography to obtain pure solid compounds ***5a-5b*** in 65−69% yields. All the newly synthesized compounds were characterized by ^{1}H NMR, ^{13}C NMR and HRMS (ESI).

6.1.1. Ethyl 3-phenyl-2-(4-(4-phenyl-1H-1,2,3-triazol-1-yl) benzamido)propanoate (***5a***)

White solid, Yield 65%; mp: 118−120 °C. ^{1}H NMR (500 MHz,

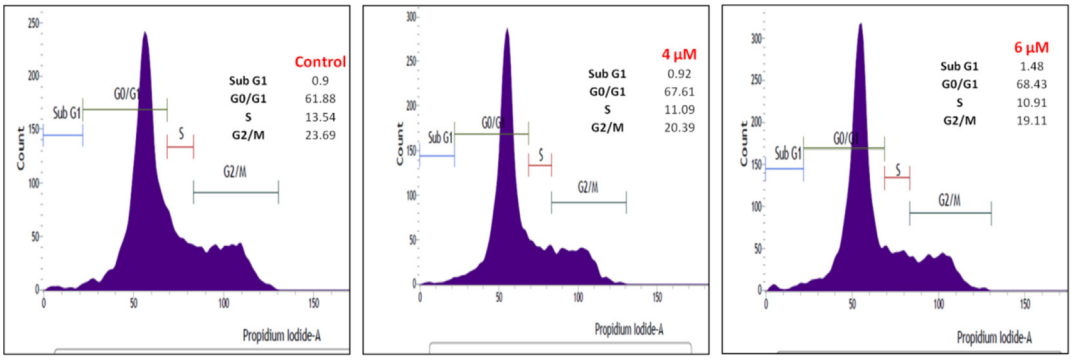

Fig. 8. Effect of **22a** on progression of MDA-MB-231 cell cycle as analysed by flow cytometry. Cells treated with 22a at concentrations of 4 and 6 μM show G0/G1 phase arrest of cell cycle.

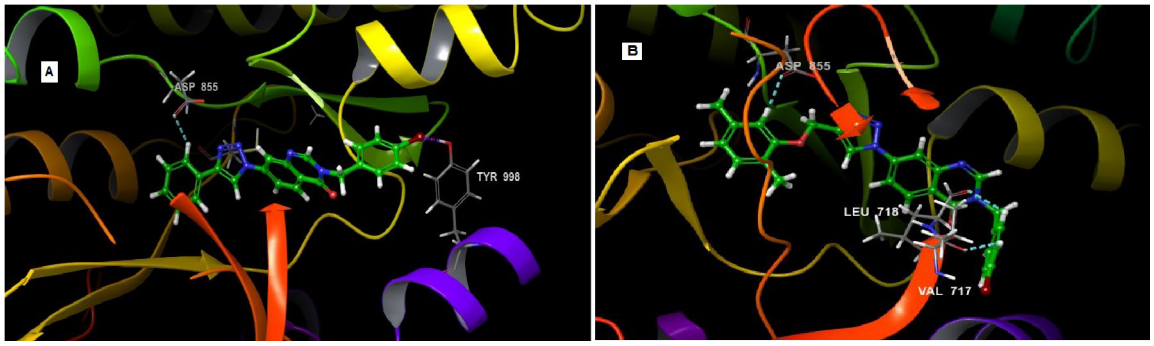

Fig. 9. (A) Interactions of compound **22a** with active site residue TYR998 and ASP855 of EGFR protein (PDB ID: 1XKK) (**B**) Interactions of compound **23b** with VAL717, LEU718 and ASP 855 of EGFR protein (PDB ID: 1XKK).

DMSO−d_6) δ 9.40 (s, 1H), 9.02 (d, J = 7.7 Hz, 1H), 8.11−8.03 (m, 4H), 7.99−7.94 (m, 2H), 7.55−7.48 (m, 2H), 7.43−7.38 (m, 1H), 7.35−7.27 (m, 4H), 7.24−7.18 (m, 1H), 4.74−7.64 (m, 1H), 4.11 (q, J = 7.1 Hz, 2H), 3.23−3.09 (m, 2H), 1.15 (t, J = 7.1 Hz, 3H) ppm; ^{13}C NMR (125 MHz, DMSO−d_6) δ 172.05, 165.84, 148.01, 139.09, 138.06, 133.97, 130.57, 129.67, 129.56, 129.51, 128.84, 128.73, 126.99, 125.88, 120.15, 120.02, 61.09, 54.96, 36.83, 14.48 ppm; HRMS (ESI): *m/z* calcd for $[M+H]^+$ $C_{26}H_{25}N_4O_3$ 441.1926; found 441.1935.

*6.1.2. Methyl 3-methyl-2-(4-(4-phenyl-1H-1,2,3-triazol-1-yl) benzamido)butanoate (**5b**)*

White solid, Yield 69%; mp: 255−257 °C. ^{1}H NMR (500 MHz, DMSO−d_6) δ 9.42 (s, 1H), 8.80 (d, J = 7.7 Hz, 1H), 8.18−8.13 (m, 2H), 8.12−8.07 (m, 2H), 8.00−7.95 (m, 2H), 7.55−7.49 (m, 2H), 7.44−7.38 (m, 1H), 4.38−4.33 (m, 1H), 3.68 (s, 3H), 2.27−2.17 (m, 1H), 1.02 (d, J = 6.7 Hz, 3H), 0.97 (d, J = 6.8 Hz, 3H) ppm; ^{13}C NMR (125 MHz, DMSO−d_6) δ 172.59, 166.37, 148.03, 139.06, 134.14, 130.58, 129.97, 129.49, 128.84, 125.89, 120.15, 119.88, 59.22, 52.15, 30.05, 19.62, 19.53 ppm; HRMS (ESI): *m/z* calcd for $[M+H]^+$ $C_{21}H_{23}N_4O_3$ 379.1770; found 379.1777.

*6.2. General reaction procedure for the synthesis of methyl 2-(2-methyl-4-oxoquinazolin-3(4H)-yl)acetate **10a-10b, 11a-11d** derivatives*

Methyl 2-(2-methyl-4-oxo-6-(prop-2-yn-1-yloxy)quinazolin-3(4H)-yl)acetate (**9**, 2 mmol) and azides or oximes (2 mmol) (Scheme 1) were mixed in a 10 mL volume of 1:1 *tert*-BuOH/H_2O mixture. To the heterogeneous mixture, sodium ascorbate (10 mol %), followed by copper(II)sulfate pentahydrate (2 mol%) were added and the reaction mixture was allowed to stir for 10-14 h to give crude white precipitates, which were filtered, washed with water, followed by hexane and finally purified by using column chromatography to obtain as pure white solid compounds **10a-10b, 11a-11d** in 84−90% yields. All the newly synthesized compounds were characterized by ^{1}H NMR, ^{13}C NMR and HRMS (ESI).

*6.2.1. Methyl 2-(6-((3-(4-chlorophenyl)isoxazol-5-yl)methoxy)-2-methyl-4-oxoquinazolin-3(4H)-yl) acetate (**10a**)*

White solid, Yield 51%; mp: 125−127 °C ^{1}H NMR (500 MHz, DMSO−d_6) δ 7.94−7.90 (m, 2H), 7.64 (d, J = 2.9 Hz, 1H), 7.62−7.57 (m, 3H), 7.57−7.53 (m, 1H), 7.24 (s, 1H), 5.49 (s, 2H), 4.94 (s, 2H), 3.72 (s, 3H), 2.50 (s, 3H) ppm; ^{13}C NMR (125 MHz, DMSO−d_6) δ 169.05, 169.04, 161.58, 161.28, 156.29, 153.27, 142.65, 135.54, 129.73, 129.12, 128.96, 127.61, 125.07, 120.69, 108.30, 102.93, 61.49, 52.96, 45.96, 23.03 ppm; HRMS (ESI): *m/z* calcd for $[M+H]^+$ $C_{22}H_{19}ClN_3O_5$ 440.1013; found 440.1016.

*6.2.2. Methyl2-(2-methyl-4-oxo-6-((3-(p-tolyl)isoxazol-5-yl) methoxy)quinazolin-3(4H)-yl)acetate (**10b**)*

White solid, Yield 74%; mp: 177−179 °C. ^{1}H NMR (500 MHz, DMSO−d_6) δ 7.81−7.75 (m, 2H), 7.66−7.60 (m, 2H), 7.57−7.53 (m, 1H), 7.35−7.30 (m, 2H), 7.18 (s, 1H), 5.48 (s, 2H), 4.94 (s, 2H), 3.73 (s, 3H), 2.50 (s, 3H), 2.37 (s, 3H) ppm; ^{13}C NMR (125 MHz, DMSO−d_6) δ 169.07, 168.52, 162.36, 161.28, 156.30, 153.27, 142.60, 140.59, 130.18, 129.11, 127.04, 125.91, 125.11, 120.65, 108.13, 102.84, 61.43, 52.99, 45.97, 23.05, 21.43 ppm; HRMS (ESI): *m/z* calcd for $[M+H]^+$ $C_{23}H_{22}N_3O_5$ 420.1559; found 420.1560.

*6.2.3. Methyl 2-(6-((1-(3-chlorophenyl)-1H-1,2,3-triazol-4-yl) methoxy)-2-methyl-4-oxoquinazolin-3(4H)-yl)acetate (**11a**)*

Yellow solid, Yield 74%; mp: 255−257 °C ^{1}H NMR (500 MHz, DMSO−d_6) δ 9.06 (s, 1H), 8.07 (t, J = 2.0 Hz, 1H), 7.96−7.92 (m, 1H), 7.68 (d, J = 2.9 Hz, 1H), 7.66−7.59 (m, 2H), 7.59−7.55 (m, 1H), 7.54−7.50 (m, 1H), 5.38 (s, 2H), 4.95 (s, 2H), 3.73 (s, 3H), 2.51 (s, 3H) ppm; ^{13}C NMR (125 MHz, DMSO−d_6) δ 169.11, 161.31, 156.71, 153.03, 144.23, 142.34, 138.03, 134.69, 132.12, 129.08, 128.99, 125.08, 123.62, 120.68, 120.44, 119.22, 108.03, 62.02, 52.98, 45.95, 23.03 ppm; HRMS (ESI): *m/z* calcd for $[M+H]^+$ $C_{22}H_{19}ClN_3O_5$ 440.1013; found 440.1019.

*6.2.4. Methyl 2-(6-((1-(4-methoxyphenyl)-1H-1,2,3-triazol-4-yl) methoxy)-2-methyl-4-oxoquinazolin-3(4H)-yl)acetate (**11b**)*

White solid, Yield 55%; mp: 135−137 °C. ^{1}H NMR (500 MHz, DMSO−d_6) δ 8.86 (s, 1H), 7.90−7.75 (m, 2H), 7.68 (d, J = 2.9 Hz, 1H), 7.60 (d, J = 8.9 Hz, 1H), 7.55−7.50 (m, 1H), 7.17−7.09 (m, 2H), 5.35 (s, 2H), 4.94 (s, 2H), 3.83 (s, 3H), 3.73 (s, 3H), 2.51 (s, 3H) ppm; ^{13}C NMR (125 MHz, DMSO−d_6) δ 169.08, 161.33, 159.84, 156.81, 152.98, 143.79, 142.33, 130.46, 128.97, 125.08, 123.40, 122.34, 120.70, 115.38, 108.11, 62.15, 56.05, 52.95, 45.94, 23.01 ppm; HRMS (ESI): *m/z* calcd for $[M+H]^+$ $C_{22}H_{22}N_5O_5$ 436.1621; found 436.1629.

*6.2.5. Methyl 2-(2-methyl-4-oxo-6-((1-(m-tolyl)-1H-1,2,3-triazol-4-yl)methoxy)quinazolin-3(4H)-yl)acetate (**11c**)*

White solid, Yield 74%; mp: 188−190 °C. ^{1}H NMR (500 MHz, DMSO−d_6) δ 8.95 (s, 1H), 7.78−7.75 (m, 1H), 7.72−7.69 (m, 1H), 7.68 (d, J = 2.9 Hz, 1H), 7.61 (d, J = 8.9 Hz, 1H), 7.55−7.51 (m, 1H), 7.49 (t, J = 7.8 Hz, 1H), 7.34−7.31 (m, 1H), 5.37 (s, 2H), 4.95 (s, 2H), 3.73 (s, 3H), 2.50 (s, 3H), 2.42 (s, 3H) ppm; ^{13}C NMR (125 MHz, DMSO−d_6) δ 169.11, 161.32, 156.76, 153.03, 143.96, 142.32, 140.17, 136.97, 130.19, 129.86, 128.99, 125.12, 123.39, 121.07, 120.68, 117.72, 108.01, 62.08, 52.98, 45.95, 23.03, 21.38 ppm; HRMS (ESI): *m/z* calcd for $[M+H]^+$ $C_{22}H_{22}N_5O_4$ 420.1672; found 420.1670.

*6.2.6. Methyl-2-(2-methyl-4-oxo-6-((1-(3,4,5-trimethylphenyl)-1H-1,2,3-triazol-4-yl)methoxy)quinazolin-3(4H)-yl)acetate (**11d**)*

White solid, Yield 64%; mp: 139–141. °C ^{1}H NMR (500 MHz, DMSO–d_6) δ 8.45 (s, 1H), 7.66 (d, J = 2.9 Hz, 1H), 7.59 (d, J = 8.9 Hz, 1H), 7.53 (dd, J = 8.9, 2.9 Hz, 1H), 7.09 (s, 2H), 5.38 (s, 2H), 4.94 (s, 2H), 3.73 (s, 3H), 2.50 (s, 3H), 2.33 (s, 3H), 1.86 (s, 6H) ppm; ^{13}C NMR (125 MHz, DMSO–d_6)) δ 169.07, 161.30, 156.76, 153.00, 142.94, 142.32, 140.02, 134.95, 133.79, 129.34, 128.91, 127.14, 125.28, 120.66, 108.49, 62.28, 52.95, 45.94, 23.01, 21.09, 17.26 ppm; HRMS (ESI): *m/z* calcd for $[M+H]^+$ $C_{24}H_{26}N_5O_4$ 448.1985; found 448.1990.

*6.3. General reaction procedure for the synthesis of 6-((1H-1,2,3-triazol-4-yl)methoxy)-3-benzyl-2-methylquinazolin-4(3H)-one **16a-16j**, and (E)-4-(2-(6-((1H-1,2,3-triazol-4-yl)methoxy)-3-benzyl-4-oxo-3,4-dihydroquinazolin-2-yl)vinyl)benzonitrile derivatives **17a-17b***

Compounds **16a**-**16j** were prepared in a similar way as procedure described above. Compound (**16**, 1 mmol) was dissolved in glacial acetic acid, to which 4-cyano benzaldehyde (1 mmol) (Scheme 2) was added and the reaction mixture was allowed to reflux for 16–18 h. The reaction was monitored by TLC. After completion of reaction, water was added to afford crude precipitates, which were filtered, washed with water, followed by cold methanol and hexane to afford a pure yellow to pale yellow products of *(E)-4-(2-(6-((1H-1,2,3-triazol*-4-yl*)methoxy)-3-benzyl-4-oxo-3,4-dihydroquinazolin*-2-yl*)vinyl)benzonitrile derivatives **17a-17b*** in 71–83% yields. All the newly synthesized compounds were characterized by ^{1}H NMR, ^{13}C NMR and HRMS (ESI).

*6.3.1. 3-benzyl-6-((1-(3-chlorophenyl)-1H-1,2,3-triazol-4-yl) methoxy)-2-methylquinazolin-4(3H)-one (**16a**)*

White solid, Yield 70%; mp: 240–242 °C. ^{1}H NMR (500 MHz, DMSO–d_6) δ 9.06 (s, 1H), 8.08 (s, 1H), 7.97–7.93 (m, 1H), 7.75 (d, J = 2.8 Hz, 1H), 7.66–7.59 (m, 2H), 7.59–7.56 (m, 1H), 7.55–7.50 (m, 1H), 7.40–7.32 (m, 2H), 7.31–7.25 (m, 1H), 7.20 (d, J = 7.6 Hz, 2H), 5.39 (s, 4H), 2.47 (s, 3H) ppm; ^{13}C NMR (125 MHz, DMSO–d_6) δ 161.74, 156.72, 153.38, 144.31, 142.47, 138.08, 137.04, 134.70, 132.11, 129.26, 129.08, 128.96, 127.77, 126.77, 124.91, 123.60, 121.13, 120.49, 119.27, 108.39, 62.11, 46.91, 23.16 ppm; HRMS (ESI): *m/z* calcd for $[M+H]^+$ $C_{25}H_{21}ClN_5O_2$ 458.1384; found 458.1384.

*6.3.2. 3-benzyl-6-((1-(4-chlorophenyl)-1H-1,2,3-triazol-4-yl) methoxy)-2-methylquinazolin-4(3H)-one (**16b**)*

White solid, Yield 74%; mp: 235–237 °C. ^{1}H NMR (500 MHz, DMSO–d_6) δ 9.01 (s, 1H), 8.02–7.93 (m, 2H), 7.75 (d, J = 2.8 Hz, 1H), 7.71–7.66 (m, 2H), 7.63–7.58 (m, 1H), 7.52 (dd, J = 8.9, 2.9 Hz, 1H), 7.39–7.32 (m, 2H), 7.31–7.25 (m, 1H), 7.20 (d, J = 7.4 Hz, 2H), 5.39 (s, 4H), 2.47 (s, 3H) ppm; ^{13}C NMR (125 MHz, DMSO–d_6) δ 161.73, 156.73, 153.36, 144.28, 142.46, 137.03, 135.84, 133.56, 130.35, 129.26, 128.95, 127.77, 126.76, 124.91, 123.51, 122.35, 121.12, 108.34, 62.08, 46.91, 23.16 ppm; HRMS (ESI): *m/z* calcd for $[M+H]^+$ $C_{25}H_{21}ClN_5O_2$ 458.1384; found 458.1387.

*6.3.3. 3-benzyl-2-methyl-6-((1-(m-tolyl)-1H-1,2,3-triazol-4-yl) methoxy)quinazolin-4(3H)-one (**16c**)*

White solid, Yield 58%; mp: 215–217 °C. ^{1}H NMR (500 MHz, DMSO-d_6) δ 8.95 (s, 1H), 7.77 (s, 1H), 7.75 (d, J = 2.8 Hz, 1H), 7.73–7.69 (m, 1H), 7.61 (d, J = 8.9 Hz, 1H), 7.53 (dd, J = 8.9, 2.8 Hz, 1H), 7.48 (t, J = 7.8 Hz, 1H), 7.39–7.25 (m, 4H), 7.20 (d, J = 7.6 Hz, 2H), 5.39 (s, 2H), 5.38 (s, 2H), 2.47 (s, 3H), 2.42 (s, 3H) ppm; ^{13}C NMR (125 MHz, DMSO-d_6) δ 161.75, 156.77, 153.36, 144.04, 142.45, 140.16, 137.04, 137.02, 130.17, 129.84, 129.26, 128.95, 127.77, 126.77, 124.93, 123.35, 121.13, 121.10, 117.75, 108.33, 62.16, 46.91, 23.16, 21.37 ppm; HRMS (ESI): *m/z* calcd for $[M+H]^+$ $C_{26}H_{24}N_5O_2$ 438.1930; found 438.1931.

*6.3.4. 3-benzyl-6-((1-(3-chloro-4-fluorophenyl)-1H-1,2,3-triazol-4-yl)methoxy)-2-methylquinazolin-4(3H)-one (**16d**)*

White solid, Yield 62%; mp: 195–197 °C. ^{1}H NMR (500 MHz, DMSO-d_6) δ 9.02 (s, 1H), 8.25 (dd, J = 6.3, 2.6 Hz, 1H), 8.02–7.96 (m, 1H), 7.75 (d, J = 2.8 Hz, 1H), 7.72–7.66 (m, 1H), 7.63–7.58 (m, 1H), 7.54–7.50 (m, 1H), 7.39–7.32 (m, 2H), 7.31–7.26 (m, 1H), 7.20 (d, J = 7.5 Hz, 2H), 5.39 (s, 4H), 2.47 (s, 3H) ppm; ^{13}C NMR (125 MHz, DMSO-d_6) δ 161.73, 158.42, 156.72, 156.45, 153.38, 144.32, 142.47, 137.04, 134.04, 129.26, 128.96, 127.77, 126.77, 124.89, 123.78, 123.04, 121.57, 121.13, 118.71, 108.39, 62.10, 46.92, 23.16. HRMS (ESI): *m/z* calcd for $[M+H]^+$ $C_{25}H_{20}FClN_5O_2$ 476.1289; found 476.1294.

*6.3.5. 3-benzyl-2-methyl-6-((1-(2-methyl-4-nitrophenyl)-1H-1,2,3-triazol-4-yl)methoxy)quinazolin-4(3H)-one (**16e**)*

Pale yellow solid, Yield 79%; mp: 205–207 °C. ^{1}H NMR (500 MHz, DMSO-d_6) δ 8.81 (s, 1H), 8.40 (d, J = 11.3 Hz, 1H), 8.30–8.19 (m, 1H), 7.84–7.72 (m, 2H), 7.66–7.49 (m, 2H), 7.40–7.32 (m, 3H), 7.32–7.25 (m, 1H), 7.20 (d, J = 7.3 Hz, 1H), 5.42 (s, 2H), 5.39 (s, 2H), 2.47 (s, 3H), 2.35 (s, 3H) ppm; ^{13}C NMR (125 MHz, DMSO-d_6) δ ^{13}C NMR (125 MHz, DMSO) δ 161.74, 156.73, 153.39, 148.06, 143.51, 142.46, 141.30, 137.03, 135.61, 129.26, 128.94, 127.78, 127.76, 126.91, 126.87, 126.77, 125.00, 122.70, 121.10, 108.40, 62.00, 46.91, 23.16, 18.30 ppm; HRMS (ESI): *m/z* calcd for $[M+H]^+$ $C_{26}H_{23}N_6O_4$ 483.1781; found 483.1785.

*6.3.6. 3-benzyl-2-methyl-6-((1-(3,4,5-trimethylphenyl)-1H-1,2,3-triazol-4-yl)methoxy)quinazolin-4(3H)-one (**16f**)*

White solid, Yield 75%; mp: 165–167 °C. ^{1}H NMR (500 MHz, DMSO-d_6) δ 8.46 (s, 1H), 7.74 (d, J = 2.6 Hz, 1H), 7.59 (d, J = 8.9 Hz, 1H), 7.53 (dd, J = 8.9, 2.7 Hz, 1H), 7.39–7.32 (m, 2H), 7.32–7.26 (m, 1H), 7.19 (d, J = 7.5 Hz, 2H), 7.09 (s, 2H), 5.40 (s, 2H), 5.39 (s, 2H), 2.47 (s, 3H), 2.33 (s, 3H), 1.87 (s, 6H) ppm; ^{13}C NMR (125 MHz, DMSO-d_6) δ 161.71, 156.70, 153.34, 142.99, 142.41, 140.01, 137.04, 134.94, 133.78, 129.33, 129.25, 128.87, 127.78, 127.12, 126.76, 125.15, 121.06, 108.66, 62.27, 46.89, 23.15, 21.09, 17.26 ppm; HRMS (ESI): *m/z* calcd for $[M+H]^+$ $C_{28}H_{28}N_5O_2$ 466.2243; found 466.2243.

*6.3.7. 3-benzyl-2-methyl-6-((1-(3,4,5-trimethoxyphenyl)-1H-1,2,3-triazol-4-yl)methoxy)quinazolin-4(3H)-one (**16g**)*

White solid, Yield 77%; mp: 255–257 °C. ^{1}H NMR (500 MHz, DMSO-d_6) δ 9.00 (s, 1H), 7.75 (d, J = 2.9 Hz, 1H), 7.61 (d, J = 8.9 Hz, 1H), 7.52 (dd, J = 8.9, 2.9 Hz, 1H), 7.38–7.33 (m, 2H), 7.31–7.26 (m, 1H), 7.24 (s, 2H), 7.21–7.17 (m, 2H), 5.39 (s, 4H), 3.88 (s, 6H), 3.72 (s, 3H), 2.47 (s, 3H) ppm; ^{13}C NMR (125 MHz, DMSO-d_6) δ 161.74, 156.76, 154.02, 153.38, 143.95, 142.46, 138.01, 137.04, 132.90, 129.26, 128.95, 127.78, 126.76, 124.95, 123.69, 121.12, 108.35, 98.78, 62.23, 60.68, 56.82, 46.92, 23.16 ppm; HRMS (ESI): *m/z* calcd for $[M+H]^+$ $C_{28}H_{28}N_5O_5$ 514.2090; found 514.2095.

*6.3.8. 3-benzyl-6-((1-benzyl-1H-1,2,3-triazol-4-yl)methoxy)-2-methylquinazolin-4(3H)-one (**16h**)*

White solid, Yield 70%; mp: 155–157 °C. ^{1}H NMR (500 MHz, DMSO-d_6) δ 8.31 (s, 1H), 7.69 (d, J = 2.9 Hz, 1H), 7.58 (d, J = 8.9 Hz, 1H), 7.48 (dd, J = 8.9, 2.9 Hz, 1H), 7.39–7.27 (m, 8H), 7.22–7.17 (m, 2H), 5.62 (s, 2H), 5.39 (s, 2H), 5.28 (s, 2H), 2.47 (s, 3H) ppm; ^{13}C NMR (125 MHz, DMSO-d_6) δ 161.66, 156.82, 153.46, 143.16, 142.12, 136.99, 136.46, 129.25, 129.23, 128.70, 128.62, 128.42, 127.78, 126.78, 125.24, 125.02, 121.05, 108.29, 62.17, 53.34, 46.94, 23.08 ppm; HRMS (ESI): *m/z* calcd for $[M+H]^+$ $C_{26}H_{24}N_5O_2$ 438.1930; found 438.1934.

*6.3.9. 3-benzyl-6-((1-(4-bromobenzyl)-1H-1,2,3-triazol-4-yl) methoxy)-2-methylquinazolin-4(3H)-one (**16i**)*

White solid, Yield 55%; mp: 175–177 °C. ^{1}H NMR (500 MHz,

DMSO-d_6) δ 8.31 (s, 1H), 7.69 (d, J = 2.9 Hz, 1H), 7.60–7.54 (m, 3H), 7.47 (dd, J = 8.9, 2.9 Hz, 1H), 7.38–7.33 (m, 2H), 7.31–7.26 (m, 3H), 7.21–7.17 (m, 2H), 5.61 (s, 2H), 5.38 (s, 2H), 5.28 (s, 2H), 2.46 (s, 3H) ppm; ^{13}C NMR (125 MHz, DMSO-d_6) δ 161.71, 156.77, 153.34, 143.22, 142.32, 137.02, 135.86, 132.17, 130.68, 129.26, 128.85, 127.78, 126.76, 125.32, 124.99, 121.91, 121.06, 108.25, 62.13, 52.58, 46.91, 23.14 ppm; HRMS (ESI): *m/z* calcd for $[M+H]^+$ $C_{26}H_{23}BrN_5O_2$ 516.1035; found 516.1037.

*6.3.10. 3-benzyl-2-methyl-6-((1-(4-nitrobenzyl)-1H-1,2,3-triazol-4-yl)methoxy)quinazolin-4(3H)-one (**16j**)*

White solid, Yield 76%; mp: 254–256 °C. ^{1}H NMR (500 MHz, DMSO-d_6) δ 8.39 (s, 1H), 8.25–8.22 (m, 2H), 7.70 (d, J = 2.9 Hz, 1H), 7.62–7.58 (m, 1H), 7.55–7.51 (m, 2H), 7.51–7.47 (m, 1H), 7.38–7.32 (m, 2H), 7.31–7.26 (m, 1H), 7.22–7.18 (m, 2H), 5.82 (s, 2H), 5.39 (s, 2H), 5.31 (s, 2H), 2.49 (s, 3H) ppm; ^{13}C NMR (125 MHz, DMSO-d_6) δ 161.51, 156.88, 153.92, 147.75, 143.84, 143.32, 141.48, 136.83, 129.51, 129.25, 128.26, 127.82, 126.82, 125.70, 125.15, 124.38, 120.98, 108.45, 62.17, 52.44, 47.03, 22.87 ppm; HRMS (ESI): *m/z* calcd for $[M+H]^+$ $C_{22}H_{23}N_6O_4$ 483.1781; found 483.1785.

*6.3.11. (E)-4-(2-(3-benzyl-6-((1-(3-chlorophenyl)-1H-1,2,3-triazol-4-yl)methoxy)-4-oxo-3,4-dihydroquinazolin-2-yl)vinyl)benzonitrile (**17a**)*

Yellow solid, Yield 68%; mp: 200–202 °C. ^{1}H NMR (500 MHz, DMSO–d_6) δ 9.08 (s, 1H), 8.08 (t, J = 2.0 Hz, 1H), 7.98–7.93 (m, 1H), 7.89–7.84 (m, 4H), 7.84–7.78 (m, 2H), 7.73 (d, J = 8.9 Hz, 1H), 7.65 (t, J = 8.1 Hz, 1H), 7.60–7.55 (m, 2H), 7.53 (d, J = 15.4 Hz, 1H), 7.35–7.30 (m, 2H), 7.29–7.21 (m, 3H), 5.68 (s, 2H), 5.42 (s, 2H) ppm; ^{13}C NMR (125 MHz, DMSO–d_6) δ 161.60, 157.20, 150.10, 144.22, 142.31, 140.20, 138.05, 137.71, 137.68, 134.70, 133.19, 132.13, 129.66, 129.22, 129.10, 128.95, 127.84, 127.04, 125.23, 123.94, 123.66, 121.45, 120.47, 119.25, 119.17, 111.86, 108.52, 62.11, 45.76 ppm; HRMS (ESI): *m/z* calcd for $[M+H]^+$ $C_{33}H_{24}ClN_6O_2$ 571.1649; found 571.1650.

*6.3.12. (E)-4-(2-(3-benzyl-6-((1-(3-chloro-4-fluorophenyl)-1H-1,2,3-triazol-4-yl)methoxy)-4-oxo-3,4-dihydroquinazolin-2-yl)vinyl)benzonitrile (**17b**)*

Yellow solid, Yield 64%; mp: 229–231 °C; ^{1}H NMR (500 MHz, DMSO–d_6) δ 9.04 (s, 1H), 8.28–8.24 (m, 1H), 8.03–7.97 (m, 1H), 7.91–7.84 (m, 4H), 7.84–7.78 (m, 2H), 7.76–7.66 (m, 2H), 7.60–7.50 (m, 2H), 7.35–7.30 (m, 2H), 7.30–7.20 (m, 3H), 5.68 (s, 2H), 5.43 (s, 2H) ppm; ^{13}C NMR (125 MHz, DMSO–d_6) δ 161.61, 157.20, 150.12, 144.24, 142.32, 140.21, 137.72, 137.68, 134.04, 134.01, 133.20, 129.68, 129.27, 129.22, 128.96, 127.85, 127.04, 125.24, 123.96, 123.86, 123.04, 121.58, 121.52, 121.46, 121.36, 121.21, 119.17, 118.74, 118.56, 111.87, 108.54, 62.10, 45.76 ppm; HRMS (ESI): *m/z* calcd for $[M+H]^+$ $C_{33}H_{23}ClFN_6O_2$ 589.1555; found 589.1563.

*6.4. General reaction procedure for the synthesis of 2-methyl-3-1H-1,2,3-triazol-1-yl)phenyl)quinazolin-4(3H)-one derivatives **22a-22b, 22'a** and **23a-23d***

6 or 7-azido-3-benzylquinazolin-4(3*H*)-one (**21**, 2 mmol) and phenylacetylene or phenoxyacetylenes (2 mmol) (Scheme 3) were mixed in a 10 mL volume of 1:1 *tert*-BuOH/H_2O mixture. To the heterogeneous mixture, sodium ascorbate (10 mol%), followed by copper(II)sulfate pentahydrate (2 mol%) were added and the reaction mixture was allowed to stir for 12-14 h to give crude white precipitates, which were filtered, washed with water, followed by hexane and finally purified by using column chromatography to obtain as pure white solid compounds **22a-22b**, **22'a** and **23a-23d** in 84–90% yields. All the newly synthesized compounds were characterized by ^{1}H NMR, ^{13}C NMR and HRMS (ESI).

*6.4.1. 3-(4-bromobenzyl)-7-(4-phenyl-1H-1,2,3-triazol-1-yl) quinazolin-4(3H)-one (**22a**)*

White solid, Yield 74%; mp: 215–217 °C; ^{1}H NMR (500 MHz, DMSO-d_6) δ 9.57 (s, 1H), 8.71 (s, 1H), 8.37 (d, J = 8.7 Hz, 1H), 8.29 (d, J = 2.0 Hz, 1H), 8.21 (dd, J = 8.7, 2.1 Hz, 1H), 8.01–7.94 (m, 2H), 7.60–7.55 (m, 2H), 7.55–7.49 (m, 2H), 7.44–7.35 (m, 3H), 5.21 (s, 2H) ppm; ^{13}C NMR (125 MHz, DMSO-d_6) δ 159.99, 150.00, 149.67, 148.21, 141.23, 136.51, 132.03, 130.54, 130.44, 129.53, 129.07, 128.94, 125.91, 121.64, 121.43, 120.41, 118.97, 117.42, 49.07 ppm; HRMS (ESI): *m/z* calcd for $[M+H]^+$ $C_{23}H_{17}BrN_5O$ 458.0616; found 458.0618.

*6.4.2. 3-(4-bromobenzyl)-7-(4-(p-tolyl)-1H-1,2,3-triazol-1-yl) quinazolin-4(3H)-one (**22b**)*

White solid, Yield 64%; mp: 200–202 °C. ^{1}H NMR (500 MHz, DMSO-d_6) δ 9.51 (s, 1H), 8.70 (s, 1H), 8.37 (d, J = 8.7 Hz, 1H), 8.28 (d, J = 2.1 Hz, 1H), 8.20 (dd, J = 8.7, 2.2 Hz, 1H), 7.88–7.82 (m, 2H), 7.59–7.54 (m, 2H), 7.40–7.36 (m, 2H), 7.36–7.31 (m, 2H), 5.21 (s, 2H), 2.37 (s, 3H) ppm; ^{13}C NMR (125 MHz, TFA) δ 159.37, 154.52, 148.54, 147.57, 143.18, 139.91, 135.14, 134.23, 132.97, 132.88, 132.18, 128.89, 126.95, 125.23, 124.10, 119.71, 118.26, 116.01, 55.01, 22.06 ppm; HRMS (ESI): *m/z* calcd for $[M+H]^+$ $C_{24}H_{19}BrN_5O$ 472.0773; found 472.0774.

*6.4.3. 3-benzyl-6-(4-phenyl-1H-1,2,3-triazol-1-yl)quinazolin-4(3H)-one (**22'a**)*

White solid, Yield 75%; mp: 155–157 °C. ^{1}H NMR (500 MHz, DMSO-d_6) δ 9.55 (s, 1H), 8.69 (s, 1H), 8.66 (d, J = 2.5 Hz, 1H), 8.45 (dd, J = 8.8, 2.6 Hz, 1H), 8.02–7.93 (m, 3H), 7.54–7.48 (m, 2H), 7.44–7.35 (m, 5H), 7.34–7.29 (m, 1H), 5.27 (s, 2H) ppm; ^{13}C NMR (125 MHz, DMSO-d_6) δ 160.25, 149.19, 148.07, 137.06, 135.39, 130.58, 129.88, 129.48, 129.15, 128.80, 128.25, 128.23, 126.45, 125.86, 123.02, 120.60, 120.31, 116.86, 49.59 ppm; HRMS (ESI): *m/z* calcd for $[M+H]^+$ $C_{23}H_{18}N_5O$ 380.1511; found 380.1514.

*6.4.4. 3-benzyl-7-(4-(phenoxymethyl)-1H-1,2,3-triazol-1-yl) quinazolin-4(3H)-one (**23a**)*

White solid, Yield 79%; mp: 200–202 °C. ^{1}H NMR (500 MHz, DMSO-d_6) δ 9.22 (s, 1H), 8.70 (s, 1H), 8.35 (d, J = 8.7 Hz, 1H), 8.25 (d, J = 1.4 Hz, 1H), 8.17 (dd, J = 8.7, 1.6 Hz, 1H), 7.43–7.28 (m, 7H), 7.10 (d, J = 8.2 Hz, 2H), 6.98 (t, J = 7.3 Hz, 1H), 5.27 (s, 2H), 5.24 (s, 2H) ppm; ^{13}C NMR (125 MHz, DMSO-d_6) δ ^{13}C NMR (125 MHz, DMSO) δ 159.96, 158.45, 150.00, 149.59, 144.91, 141.10, 137.09, 130.03, 129.14, 128.99, 128.22, 128.19, 123.65, 121.69, 121.49, 119.07, 117.62, 115.23, 61.39, 49.52 ppm; HRMS (ESI): *m/z* calcd for $[M+H]^+$ $C_{24}H_{20}N_5O_2$ 410.1617; found 410.1619.

*6.4.5. 3-(4-bromobenzyl)-7-(4-((2,5-dimethylphenoxy)methyl)-1H-1,2,3-triazol-1-yl)quinazolin-4(3H)-one (**23b**)*

White solid, Yield 61%; mp: 233–235 °C. ^{1}H NMR (500 MHz, DMSO-d_6) δ 9.20 (s, 1H), 8.70 (s, 1H), 8.34 (d, J = 8.7 Hz, 1H), 8.29 (d, J = 2.0 Hz, 1H), 8.19 (dd, J = 8.7, 2.1 Hz, 1H), 7.59–7.53 (m, 2H), 7.40–7.34 (m, 2H), 7.02 (d, J = 7.5 Hz, 1H), 7.00 (s, 1H), 6.69 (d, J = 7.4 Hz, 1H), 5.24 (s, 2H), 5.20 (s, 2H), 2.29 (s, 3H), 2.12 (s, 3H) ppm; ^{13}C NMR (125 MHz, DMSO-d_6) δ 159.99, 156.47, 149.94, 149.61, 145.37, 141.18, 136.66, 136.50, 132.02, 130.74, 130.53, 128.98, 123.36, 121.75, 121.67, 121.43, 119.15, 117.63, 113.27, 61.75, 49.07, 21.52, 16.15 ppm; HRMS (ESI): *m/z* calcd for $[M+H]^+$ $C_{26}H_{23}BrN_5O_2$ 516.1035; found 516.1039.

*6.4.6. 3-(4-bromobenzyl)-7-(4-((5-ethyl-2-methoxyphenoxy) methyl)-1H-1,2,3-triazol-1-yl)quinazolin-4(3H)-one (**23c**)*

White solid, Yield 74%; mp: 265–267 °C. ^{1}H NMR (500 MHz, DMSO-d_6) δ 9.19 (s, 1H), 8.69 (s, 1H), 8.34 (d, J = 8.7 Hz, 1H), 8.26 (d, J = 1.6 Hz, 1H), 8.17 (dd, J = 8.7, 1.8 Hz, 1H), 7.56 (d, J = 8.3 Hz, 2H),

7.37 (d, $J = 8.3$ Hz, 2H), 7.06 (d, $J = 8.1$ Hz, 1H), 6.84 (s, 1H), 6.75–6.70 (m, 1H), 5.20 (s, 2H), 5.18 (s, 2H), 3.75 (s, 3H), 2.55 (q, 2H), 1.17 (t, $J = 7.6$ Hz, 3H) ppm; ^{13}C NMR (125 MHz, DMSO-d_6) δ 159.97, 149.92, 149.69, 149.60, 145.90, 145.09, 141.16, 137.88, 136.48, 132.01, 130.51, 128.98, 123.71, 121.66, 121.42, 119.84, 119.11, 117.61, 114.98, 112.68, 62.40, 55.95, 49.06, 28.26, 16.20 ppm; HRMS (ESI): *m/z* calcd for $[M+H]^+$ $C_{27}H_{25}BrN_5O_3$ 546.1141; found 546.1145.

*6.4.7. 3-(4-bromobenzyl)-7-(4-((4-(tert-pentyl)phenoxy)methyl)-1H-1,2,3-triazol-1- yl)quinazolin-4(3H)-one (**23d**)*

White solid, Yield 66%; mp: 245–247 °C. ^{1}H NMR (500 MHz, DMSO-d_6) δ 9.21 (s, 1H), 8.70 (s, 1H), 8.34 (d, $J = 8.7$ Hz, 1H), 8.26 (d, $J = 2.1$ Hz, 1H), 8.17 (dd, $J = 8.7$, 2.1 Hz, 1H), 7.64–7.51 (m, 2H), 7.39–7.35 (m, 2H), 7.28–7.24 (m, 1H), 7.04–7.00 (m, 1H), 5.23 (s, 2H), 5.20 (s, 2H), 1.58 (q, $J = 7.4$ Hz, 2H), 1.22 (s, 6H), 0.62 (t, $J = 7.4$ Hz, 3H) ppm; ^{13}C NMR (125 MHz, DMSO-d_6) δ 159.97, 156.17, 149.95, 149.61, 145.10, 141.86, 141.16, 136.49, 132.01, 130.52, 128.99, 127.26, 123.59, 121.67, 121.42, 119.12, 117.62, 114.65, 61.43, 49.06, 37.41, 36.72, 28.89, 9.52 ppm; HRMS (ESI): *m/z* calcd for $[M+H]^+$ $C_{29}H_{29}BrN_5O_2$ 558.1504; found 558.1508.

7. Pharmacology

7.1. Cell cultures

MDA-MB-231, MCF-7 (breast cancer), HCT-116, HT-29 (colon cancer) and A549 (lung cancer) were procured from National Centre for Cell Science (NCCS) Pune, India. MDA-MB-231, MCF-7, HCT-116 and HT-29 were grown in DMEM (Dulbecco Modified Eagle medium, Himedia) and A549 was grown in RPMI (Roswell Park Memorial Institute medium, Himedia) supplemented with 10% fetal bovine serum and 1% antibiotic-antimycotic solution (Sigma) in a CO_2 incubator with 5% CO_2 and 95% relative humidity at 37 °C. When the cells reached 70–75% confluence, they were treated with 0.25% trypsin/1 mM EDTA solution for further passage.

7.2. Cytotoxicity assay

Newly synthesized compounds were evaluated for cytotoxicity by 3-(4,5-dimethylthiazol-2-yl)-2,5-diphenyl tetrazolium bromide (MTT) assay in the above mentioned five cell lines. Doxorubicin was used as a reference standard. Briefly, cells were seeded in 96 well microculture plates at a density of 5×10^3 in 100 μL of media per well. The following day, cells were treated with respective compounds dissolved in DMSO for 48 h at 37 °C in a CO_2 incubator. Post incubation, media was discarded and MTT was added to all the wells at a concentration of 0.5 mg/mL (100 μL/well) followed by 4 h incubation. Further, MTT was discarded and the formazan crystals so formed were dissolved by adding 200 μL of DMSO to each well. Absorbance was recorded at 570 nm wavelength using a spectrophotometer and the percentage of growth inhibition was calculated. The tested compounds which exhibited >50% inhibition of cell viability at 10 μM in preliminary screening were further selected to evaluate the drug response curve (DRC). IC_{50} values for these selected compounds were determined from the DRC plot by linear regression method: % cell inhibition (from control optical density) versus different concentrations (in μM).

7.3. Scratch wound assay/cell migration assay

Effect of **22a** on MDA-MB-231 cell migration was determined by scratch wound assay. Briefly, cells were seeded at a density of 1×10^5 in a 6 well plate. The following day, artificial wound was created by disrupting monolayer of cells with a sterile 200 μL tip across the centre of the well. Wells were washed with sterile phosphate buffer saline (PBS) to remove detached cells and fresh culture media supplemented with Fetal bovine serum (FBS) was added. Then, the cells were treated with **22a** at doses of 2, 4 and 6 μM accordingly. Representative photographs of the artificially created gap were captured by camera (Carl Zeiss phase contrast microscope) at 0 h and 24 h post incubation and were evaluated using image analyzing software.

7.4. Acridine orange-ethidium bromide (AO-EB) staining

MDA-MB-231 cells were plated at a density of 5×10^3 cells in a 12 well plate and allowed to adhere overnight. The following day, cells were treated with **22a** at concentration of 2, 4 and 6 μM and incubated for 48 h. After 48 h, fluorescent dyes AO and EB each were added into wells and cells were observed under fluorescence microscope immediately. Representative images of all groups were captured using microscope (Nikon, Inc. Japan) at excitation of 488 nm and emission of 550 nm using 20X objective lens.

7.5. DAPI nuclear staining

MDA-MB-231 cells were seeded at a density of 5×10^3 cells. Next day, cells were treated with different concentrations of **22a** (2, 4 and 6 μM) and incubated for 48 h. Post incubation, cells were washed with PBS and permeabilized using PBS containing 0.1% Tween-20. Further, cells were fixed with 4% paraformaldehyde followed by staining with DAPI. Representative images for nuclear morphological changes induced by **22a** were captured by fluorescence microscope (Nikon, Japan) with excitation of 359 nm and emission of 461 nm using 20X objective lens.

7.6. Cell cycle analysis

To perform cell cycle analysis assay, the following procedure was followed. Briefly, MDA-MB-231 cells at a density of 1×10^6 cells/well in 6 well plate followed by treatment with **22a** at concentrations of 4 and 6 μM. 24 hrs post incubation with **22a**, cells were harvested by trypsinisation and fixed with 70% ethanol for 30 min at 4 °C. After fixation, cells were again washed with PBS and stained with propidium iodide staining buffer for 15 min in dark at room temperature. Then, the samples were analysed for propidium iodide fluorescence by flow cytometry using BD Accuri C6 flow-cytometer.

7.7. Colony formation assay

MDA-MB-231 cells were seeded at a density of 250 cells/well in a 12 well plate. After cells adhered to the culture well plate, cells were treated with different concentrations of **22a** (2, 4 and 6 μM) for 24 h. Post incubation, media was discarded and the cells were maintained in media containing Fetal bovine serum (FBS) to form colonies for a period of 10 days. After 10 days, the so called colonies were stained with 0.5% crystal violet stain. Then, the plate was imaged and colonies were counted using Vilber Fusion Fx software (Vilber Lourmat, France). The results are represented as total colony number vs. concentration.

8. Computational studies

The 3D crystal coordinates of EGFR were downloaded from the PDB and were prepared according to protocols specified in Protein Preparation Wizard of Schrödinger suite 2017. Briefly, hydrogens were added, bond orders were assigned, water molecules were removed within 5 Å distance and minimization done using OPLS-2005 force field. Compounds 11b, 11d, 16h, 17b, 22a and 23b were

drawn and converted to 3D using LigPrep, module of Schrödinger suite 2017. Further Grid has been generated with 10 Å around co-crystal and flexible ligand docking protocol has been performed by Glide, module of Schrödinger suite 2017. Fifteen conformations were generated for each compound and based on docking score and interactions, the final poses were selected. Docking protocol was optimized by calculating the RMSD of crystal and docked pose of co-crystal ligand with <1 Å [38].

Competing financial interests

The authors declare no competing financial interests.

Acknowledgements

G. S. conveys cordial thanks to DoP, Ministry of Chemicals & Fertilizers, Govt. of India, for the award of NIPER fellowship. GS and SN gratefully acknowledges Department of science and technology Govt. of India for research grant (EMR/2017/000220).

Abbreviations

CuAAC	Cu(I)- catalyzed azide-alkyne cycloaddition;
DMF	Dimethylformamide
DAPI	4,6-Diamidino-2-phenylindole
MTT	3-(4,5-dimethylthiazol-2-yl)-2,5-diphenyltetrazolium bromide
PBS	Phosphate Buffered Saline
FBS	Fetal bovine serum
AO-EB	acridine orange/ethidium bromide
DRC	Drug response curve
DOX	Doxorubicin
MDA-MB-231	triple negative breast cancer cell line.

References

[1] (a) W.J. Curran, New chemotherapeutic agents: update of major chemo-radiation trials in solid tumors, Oncology 63 (2002) 29–38;
(b) S. Fulda, Tumor resistance to apoptosis, Int. J. Cancer 124 (2009) 511–515;
(c) S. Fulda, K.M. Debatin, Extrinsic versus intrinsic apoptosis pathways in anticancer chemotherapy, Oncogene 25 (2006) 4798–4811.

[2] (a) S.W. Fesik, Promoting apoptosis as a strategy for cancer drug discovery, Nat. Rev. Cancer 5 (2005) 876–885;
(b) J.L. Fox, M. MacFarlane, Targeting cell death signalling in cancer: minimising 'Collateral damage, Br. J. Canc. 115 (2016) 5–11;
(c) I.M. Ghobrial, T.E. Witzig, A.A. Adjei, Targeting apoptosis pathways in cancer therapy, CA: Cancer J. Clin. 55 (2005) 178–194.

[3] (a) B. Dash, S. Dash, D. Laloo, C. Medhi, Design, synthesis and preliminary pharmacological screening (antimicrobial, analgesic and anti-inflammatory activity) of some novel quinazoline derivatives, J. Appl. Pharm. Sci. 7 (2017) 083–096;
(b) M. Dinari, F. Gharahi, P. Asadi, Synthesis, spectroscopic characterization, antimicrobial evaluation and molecular docking study of novel triazine–quinazolinone based hybrids, J. Mol. Struct. 1156 (2018) 43–50;
(c) N. Jain, J. Jaiswal, A. Pathak, P.K. Singour, Synthesis, Molecular Docking and Evaluation of 3-{4-[2-amino-4-(substitutedphenyl)-2H-[1,3]oxazin/thiazin-6-yl}2-phenyl-3*H*-quinazolin-4-one derivatives for their anticonvulsant activity, Cent. Nerv. Syst. Agents Med. Chem. 18 (2018) 63–73.

[4] (a) A.M. Alaa, L.A. Abou-Zeid, K.E.H. ElTahir, R.R. Ayyad, A.-A. Magda, A.S. El-Azab, Synthesis, anti-inflammatory, analgesic, COX-1/2 inhibitory activities and molecular docking studies of substituted 2-mercapto-4 (3H)-quinazolinones, Eur. J. Med. Chem. 121 (2016) 410–421;
(b) L. Yang, S. Ge, J. Huang, X. Bao, Synthesis of novel (*E*)-2-(4-(1H-1, 2, 4-triazol-1-yl) styryl)-4-(alkyl/arylmethyleneoxy) quinazoline derivatives as antimicrobial agents, Mol. Divers. 22 (2018) 71–82;
(c) H.A. Abuelizz, R.A. El-Dib, M. Marzouk, R. Al-Salahi, *In vitro* evaluation of new 2-phenoxy-benzo [g][1, 2, 4] triazolo [1,5-a] quinazoline derivatives as antimicrobial agents, Microb. Pathog. 117 (2018) 60–67;
(d) H. Ighachane, M.H. Sedra, H. Lazrek, Synthesis and evaluation of antifungal activities of (3*H*)-quinazolin-4-one derivatives against tree plant fungi, J. Mater. Environ. Sci. 8 (2017) 134–143.

[5] M. Hrast, K. Rožman, M. Jukič, D. Patin, S. Gobec, M. Sova, Synthesis and structure–activity relationship study of novel quinazolinone based inhibitors of Mur A, Bioorg. Med. Chem. Lett 27 (2017) 3529–3533.

[6] S.Y. Abbas, K.A. El-Bayouki, W.M. Basyouni, E.A. Mostafa, New series of 4 (3*H*)-quinazolinone derivatives: syntheses and evaluation of antitumor and antiviral activities, Med. Chem. Res. 27 (2018) 571–582.

[7] W. Dohle, F.L. Jourdan, G. Menchon, A.E. Prota, P.A. Foster, P. Mannion, E. Hamel, M.P. Thomas, P.G. Kasprzyk, E. Ferrandis, Quinazolinone based anticancer agents: synthesis, antiproliferative SAR, antitubulin activity, and tubulin co-crystal structure, J. Med. Chem. 61 (2018) 1031–1044.

[8] (a) C. Carmi, E. Galvani, F. Vacondio, S. Rivara, A. Lodola, S. Russo, S. Aiello, F. Bordi, G. Costantino, A. Cavazzoni, R.R. Alfieri, A. Ardizzoni, P.G. Petronini, M. Mor, Irreversible inhibition of epidermal growth factor receptor activity by 3-aminopropanamides, J. Med. Chem. 55 (2012) 2251–2264;
(b) X. Zhan, Y. Xu, Q. Qi, Y. Wang, H. Shi, Z. Mao, Synthesis, cytotoxic, and antibacterial evaluation of quinazolinone derivatives with substituted amino moiety, Chem. Biodivers. 15 (2018), e1700513.

[9] R.R. Furman, J.P. Sharman, S.E. Coutre, B.D. Cheson, J.M. Pagel, P. Hillmen, J.C. Barrientos, A.D. Zelenetz, T.J. Kipps, I. Flinn, P. Ghia, H. Eradat, T. Ervin, N. Lamanna, B. Coiffier, A.R. Pettitt, S. Ma, S. Stilgenbauer, P. Cramer, M. Aiello, D.M. Johnson, L.L. Miller, D. Li, T.M. Jahn, R.D. Dansey, M. Hallek, S.M. O'Brien, Idelalisib and rituximab in relapsed chronic lymphocytic leukemia, N. Engl. J. Med. 370 (2014) 997–1007.

[10] A.K. Gopal, B.S. Kahl, S. de Vos, N.D. Wagner-Johnston, S.J. Schuster, W.J. Jurczak, I.W. Flinn, C.R. Flowers, P. Martin, A. Viardot, K.A. Blum, A.H. Goy, A.J. Davies, P.L. Zinzani, M. Dreyling, D. Johnson, L.L. Miller, L. Holes, D. Li, R.D. Dansey, W.R. Godfrey, G.A. Salles, PI3Kδ inhibition by idelalisib in patients with relapsed indolent lymphoma, N. Engl. J. Med. 370 (2014) 1008–1018.

[11] (a) J.A. McIntyre, J. Castaner, P.A. Leeson, Canertinib Dihydrochloride, Drugs Fut. 30 (2005) 771;
(b) C.M. Galmarini, Canertinib Pfizer, IDrugs. 7 (2004) 58–63.

[12] S.L. Cao, Y.P. Feng, Y.Y. Jiang, S.Y. Liu, G.Y. Ding, R.T. Li, Synthesis and *in vitro* antitumor activity of 4(3*H*)-quinazolinone derivatives with dithiocarbamate side chains, Bioorg. Med. Chem. Lett 15 (2005) 1915–1917.

[13] S.T. Al-Rashood, I.A. Aboldahab, M.N. Nagi, L.A. Abouzeid, A.A.M. Abdel-Aziz, S.G. Abdel-hamide, K.M. Youssef, A.M. Al-Obaida, H.I. El-Subbagh, Synthesis, dihydrofolate reductase inhibition, antitumor testing, and molecular modeling study of some new 4(3*H*)-quinazolinone analogs, Bioorg. Med. Chem. 14 (2006) 8608–8621.

[14] D. Raffa, M.C. Edler, G. Daidone, B. Maggio, M. Merickech, S. Plescia, D. Schillaci, R. Bai, E. Hamel, Synthesis, cytotoxicity, and inhibitory effects on tubulin polymerization of a new 3-heterocyclo substituted 2-styrylquinazolinones, Eur. J. Med. Chem. 39 (2004) 299–304.

[15] I.A. Al-Suwaidan, A.A.M. Abdel-Aziz, T.Z. Shawer, R.R. Ayyad, A.M. Alanazi, A.M. El-Morsy, M.A. Mohamed, N.I. Abdel-Aziz, M.A.A. El-Sayed, A.S. El-Azab, Synthesis, antitumor activity and molecular docking study of some novel 3-benzyl-4(3*H*)quinazolinone analogues, J. Enzym. Inhib. Med. Chem. 31 (2015) 78–89.

[16] A. Inno, V.D. Noia, M. Martini, E. D'Argento, M.D. Salvatore, V. Arena, G. Schinzari, A. Orlandi, L.M. Larocca, A. Cassano, C. Baron, Erlotinib for patients with EGFR wild-type metastatic NSCLC: a retrospective biomarkers analysis, Pathol. Oncol. Res. 25 (2019) 513–520.

[17] L.E. Showalter, C. Oechsle, N. Ghimirey, C. Steele, B.J. Czerniecki, G.K. Koski, Th1 cytokines sensitize HER-expressing breast cancer cells to lapatinib, PLoS One 14 (2019), e0210209.

[18] S. Yin, C. Tang, B. Wang, Y. Zhang, L. Zhou, L. Xue, C. Zhang, Design, synthesis and biological evaluation of novel EGFR/HER2 dual inhibitors bearing a oxazolo[4,5-g]quinazolin-2(1H)-one scaffold, Eur. J. Med. Chem. 120 (2016) 26–36.

[19] H.R. Tsou, N. Mamuya, B.D. Johnson, M.F. Reich, B.C. Gruber, F. Ye, R. Nilakantan, R. Shen, C. Discafani, R. DeBlanc, R. Davis, F.E. Koehn, L.M. Greenberger, Y.F. Wang, A. Wissner, 6-Substituted-4-(3-bromophenylamino)quinazolines as putative irreversible inhibitors of the epidermal growth factor receptor (EGFR) and human epidermal growth factor receptor (HER-2) tyrosine kinases with enhanced antitumor activity, J. Med. Chem. 44 (2001) 2719–2734.

[20] A.M. Soliman, M. Ghorab, Exploration of *N*-alkyl-2-[(4-oxo-3-(4-sulfamoylphenyl)-3,4- dihydroquinazolin-2-yl)thio]acetamide derivatives as anticancer and radio sensitizing agents, Bioorg. Chem. 88 (2019) 102956.

[21] A.M. Soliman, A.S. Alqahtani, M. Ghorab, Novel sulphonamide benzoquinazolinones as dual EGFR/HER2 inhibitors, apoptosis inducers and Radiosensitizers, J. Enzym. Inhib. Med. Chem. 34 (2019) 1030–1040.

[22] T.S. Reddy, H. Kulhari, V.G. Reddy, A.V.S. Rao, V. Bansal, A. Kamal, R. Shukla, Synthesis and biological evaluation of pyrazolo–triazole hybrids as cytotoxic and apoptosis inducing agents, Org. Biomol. Chem. 13 (2015) 10136–10149.

[23] Y.C. Duan, Y.C. Ma, E. Zhang, X.J. Shi, M.M. Wang, X.W. Ye, H.M. Liu, Design and synthesis of novel 1,2,3-triazole-dithiocarbamate hybrids as potential anticancer agents, Eur. J. Med. Chem. 62 (2013) 11–19.

[24] A. Kamal, N. Shankaraiah, V. Devaiah, K. Laxma Reddy, A. Juvekar, S. Sen, N. Kurian, S. Zingde, Synthesis of 1,2,3-triazole-linked pyrrolobenzodiazepine conjugates employing 'click' chemistry: DNA-binding affinity and anticancer activity, Bioorg. Med. Chem. Lett 18 (2008) 1468–1473.

[25] S. Kumar, S.T. Saha, L. Gu, G. Palma, S. Perumal, A.S. Pillay, P. Singh, A. Anand, M. Kaur, V. Kumar, 1H-1,2,3-Triazole tethered Nitroimidazole–Isatin conjugates: synthesis, docking, and anti-proliferative evaluation against breast cancer, ACS Omega 3 (2018) 12106–12113.

[26] E.R. Wood, A.T. Truesdale, O.B. McDonald, D. Yuan, A. Hassel, S.H. Dickerson, B. Ellis, C. Pennisi, E. Horne, K. Lackey, K.J. Alligood, D.W. Rusnak, T.M. Gilmer,

L. Shewchuk, A unique structure for epidermal growth factor receptor bound to GW572016 (Lapatinib): relationships among protein conformation, inhibitor off-rate, and receptor activity in tumor cells, Cancer Res. 64 (2004) 6652–6659.

[27] S. Gatadi, J. Gour, M. Shukla, G. Kaul, S. Das, A. Dasgupta, Y.V. Madhavi, S. Chopra, S. Nanduri, Synthesis and evaluation of new 4-oxoquinazolin-3(4*H*)-yl)benzoic acid and benzamide derivatives as potent antibacterial agents effective against multidrug resistant *Staphylococcus aureus*, Bioorg. Chem. 83 (2018) 569–579.

[28] S. Gatadi, J. Gour, G. Kaul, M. Shukla, A. Dasgupta, R. Akunuri, R. Tripathi, Y.V. Madhavi, S. Chopra, S. Nanduri, Synthesis of new 3-phenylquinazolin-4(3*H*)-one derivatives as potent antibacterial agents effective against methicillin- and vancomycin-resistant *Staphylococcus aureus* (MRSA and VRSA), Bioorg. Chem. 81 (2018) 175–183.

[29] (a) S. Gatadi, J. Gour, M. Shukla, G. Kaul, S. Das, A. Dasgupta, S. Malasala, R.S. Borra, Y.V. Madhavi, S. Chopra, S. Nanduri, Synthesis of 1,2,3-triazole linked 4(3*H*)-Quinazolinones as potent antibacterial agents against multidrug-resistant *Staphylococcus aureus*, Eur. J. Med. Chem. 157 (2018) 1056–1067;
(b) S. Gatadi, J. Gour, M. Shukla, G. Kaul, A. Dasgupta, Y.V. Madhavi, S. Chopra, S. Nanduri, Synthesis and evaluation of new Quinazolin-4(3*H*)-one derivatives as potent antibacterial agents against multidrug resistant *Staphylococcus aureus* and *Mycobacterium tuberculosis*, Eur. J. Med. Chem. 175 (2019) 287–308.

[30] L.V. Rubinstein, R.H. Shoemaker, K.D. Paull, R.M. Simon, S. Tosini, P. Skehan, D.A. Scudiero, A. Monks, M.R. Boyd, Comparison of in vitro anticancer-drug-screening data generated with a tetrazolium assay versus a protein assay against a diverse panel of human tumor cell lines, J. Natl. Cancer Inst. 82 (1990) 1113–1117.

[31] C.C. Liang, A.Y. Park, J.-L. Guan, *In vitro* scratch assay: a convenient and inexpensive method for analysis of cell migration *in vitro*, Nat. Protoc. 2 (2007) 329–333.

[32] R. Horwitz, D. Webb, Cell migration, Curr. Biol. 13 (2003) 756–759.

[33] U.V. Mallavadhani, N.R. Vanga, M.K. Jeengar, V.G.M. Naidu, Synthesis of novel ring-A fused hybrids of oleanolic acid with capabilities to arrest cell cycle and induce apoptosis in breast cancer cells, Eur. J. Med. Chem. 74 (2014) 398–404.

[34] M.L. Barcellona, G. Cardiel, E. Gratton, Time-resolved fluorescence of DAPI in solution and bound to polydeoxynucleotides, Biochem. Biophys. Res. Commun. 170 (1990) 270–280.

[35] D.D. Von Hoff, J. Casper, E. Bradley, J. Sandbach, D. Jones, R. Makuch, Association between human tumor colony-forming assay results and response of an individual patient's tumor to chemotherapy, Am. J. Med. 70 (1981) 1027–1032.

[36] K.T. Chan, F.Y. Meng, Q. Li, C.Y. Ho, T.S. Lam, Y. To, W.H. Lee, M. Li, K.H. Chu, M. Toh, Cucurbitacin B induces apoptosis and S phase cell cycle arrest in BEL-7402 human hepatocellular carcinoma cells and is effective *via* oral administration, Cancer Lett. 294 (2010) 118–124.

[37] R. Nunez, DNA measurement and cell cycle analysis by flow cytometry, Curr. Issues Mol. Biol. 3 (2001) 67–70.

[38] (a) G.M. Sastry, M. Adzhigirey, T. Day, R. Annabhimoju, W. Sherman, Protein and ligand preparation: parameters, protocols, and influence on virtual screening enrichments, J. Comput. Aided Mol. Des. 27 (2013) 221–234;
(b) Schrödinger Release 2018-4, LigPrep, Schrödinger, LLC, New York, NY, 2018.